TIME-SERIES PHOTOMETRY OF STARS IN AND AROUND THE LAGOON NEBULA. I. ROTATION PERIODS OF 290 LOW-MASS PRE-MAIN-SEQUENCE STARS IN NGC 6530

The Astrophysical Journal, 747:51 (19pp), 2012 March 1 doi:10.1088/0004-637X/747/1/51

TIME-SERIES PHOTOMETRY OF STARS IN AND AROUND THE LAGOON NEBULA. I. ROTATION PERIODS OF 290 LOW-MASS PRE-MAIN-SEQUENCE STARS IN NGC 6530

Calen B. Henderson[1] and Keivan G. Stassun[2,3,4]
[1] Department of Astronomy, The Ohio State University, 140 W. 18th Ave., Columbus, OH 43210, USA; henderson@astronomy.ohio-state.edu
[2] Department of Physics and Astronomy, Vanderbilt University, VU Station B 1807, Nashville, TN 37235, USA
[3] Department of Physics, Fisk University, 1000 17th Ave. N., Nashville, TN 37208, USA
[4] Department of Physics, Massachusetts Institute of Technology, 77 Massachusetts Ave., Cambridge, MA 02139, USA
Received 2011 November 3; accepted 2011 December 5; published 2012 February 14

ABSTRACT

We have conducted a long-term, wide-field, high-cadence photometric monitoring survey of ∼50,000 stars in the Lagoon Nebula H II region. This first paper presents rotation periods for 290 low-mass stars in NGC 6530, the young cluster illuminating the nebula, and for which we assemble a catalog of infrared and spectroscopic disk indicators, estimated masses and ages, and X-ray luminosities. The distribution of rotation periods we measure is broadly uniform for 0.5 days $< P <$ 10 days; the short-period cutoff corresponds to breakup. We observe no obvious bimodality in the period distribution, but we do find that stars with disk signatures rotate more slowly on average. The stars' X-ray luminosities are roughly flat with rotation period, at the saturation level ($\log L_X/L_{\rm bol} \approx -3.3$). However, we find a significant positive correlation between $L_X/L_{\rm bol}$ and corotation radius, suggesting that the observed X-ray luminosities are regulated by centrifugal stripping of the stellar coronae. The period–mass relationship in NGC 6530 is broadly similar to that of the Orion Nebula Cluster (ONC), but the slope of the relationship among the slowest rotators differs from that in the ONC and other young clusters. We show that the slope of the period–mass relationship for the slowest rotators can be used as a proxy for the age of a young cluster, and we argue that NGC 6530 may be slightly younger than the ONC, making it a particularly important touchstone for models of angular momentum evolution in young, low-mass stars.

Key words: stars: individual: (NGC 6530) – stars: pre-main sequence – stars: rotation

Online-only material: color figures, extended figures, machine-readable tables

1. INTRODUCTION

Time-domain photometric monitoring surveys of young stars have been crucial to our understanding of a variety of fundamental questions related to low-mass stars in the pre-main-sequence (PMS) phase of evolution. Indeed, our empirical understanding of time-variable accretion processes (e.g., Gullbring & Gahm 1996; Bouvier et al. 1999; Stassun & Wood 1999; Bouvier et al. 2004), of magnetic activity (e.g., Walter et al. 1987; Feigelson et al. 2002, 2005, 2007; Walter et al. 2004; Stassun et al. 2004a, 2006b, 2007b), of the early evolution of stellar angular momentum (e.g., Attridge & Herbst 1992; Bouvier et al. 1993; Choi & Herbst 1996; Stassun et al. 1999; Rebull 2001; Herbst et al. 2002; Makidon et al. 2004; Lamm et al. 2005; Irwin et al. 2008a, 2008b), of the inner architectures of protoplanetary disks (e.g., Bouvier et al. 2003; Winn et al. 2006; Bouvier et al. 2007; Herbst et al. 2008, 2010), of the formation of binary stars (e.g., Mathieu et al. 1997; Basri et al. 1997; Jensen et al. 2007; Stassun et al. 2008), of outbursts (e.g., Walter et al. 2004; Briceño et al. 2004; Kastner et al. 2004; Grosso et al. 2005; Aspin et al. 2006; Aspin 2011; Covey et al. 2011; Bastien et al. 2011), of pulsations (e.g., Zwintz & Weiss 2006; Guenther et al. 2007), and of the fundamental masses and radii of PMS stars (e.g., Casey et al. 1998; Covino et al. 2000; Stassun et al. 2004b, 2006a, 2007a; Irwin et al. 2007; Stempels et al. 2008; Stassun et al. 2008; Hebb et al. 2010), has relied upon detailed light curves of T Tauri stars (TTSs) in a variety of young clusters and star-forming regions spanning a range of ages and star-forming environments.

The most extensively monitored regions include the Taurus–Auriga association (age ∼1–3 Myr), the Orion Nebula Cluster (ONC; ∼1–2 Myr), NGC 2264 (∼3 Myr), NGC 2362 (∼3–4 Myr), IC 348 (∼4–5 Myr), and NGC 2547 (∼40 Myr). At a distance of ∼400 pc (e.g., Menten et al. 2007), the ONC and the larger star-forming region surrounding it is the nearest and perhaps the single best-studied massive star-forming region. This region contributes photometrically determined rotation periods for hundreds of TTSs (see Herbst et al. 2007 and references therein), nearly all of the known PMS eclipsing binary stars (see Stassun et al. 2009 and references therein), including the only brown-dwarf eclipsing binary system yet discovered (Stassun et al. 2006a, 2007a; Gómez Maqueo Chew et al. 2009; Mohanty et al. 2009, 2010), and the most well-studied FUor/EXor-type eruptive star discovered in recent times (V1647 Ori; see, e.g., Bastien et al. 2011 and references therein). Thanks in large part to the broad array of discoveries enabled by the extensive photometric monitoring surveys of this region, the ONC has become a crucial test bed for star formation theory, from PMS angular momentum evolution (see Stassun & Terndrup 2003; Herbst et al. 2007) to the nature of the initial mass function (IMF; see Hillenbrand 1997; Da Rio et al. 2010). As wide-area photometric monitoring campaigns begin to survey a larger number of star-forming regions, particularly rich young clusters like the ONC, the discovery space is becoming enlarged for larger samples of benchmark PMS objects. For example, the recent Palomar Transient Factory surveys of the 25 Ori and North America/Pelican nebulae have already resulted in the discovery of numerous new candidate PMS eclipsing binaries and new FUor/EXor outburst systems (van Eyken et al. 2011; Covey et al. 2011).

In this paper we report the first results of a large-scale, multi-year, high-cadence photometric monitoring survey of the bright Lagoon Nebula (Messier 8) H II star-forming region. The massive star cluster illuminating the nebula, NGC 6530, includes

a rich population of $\gtrsim$1100 stellar members spanning the full IMF, from massive OB-type stars down to at least the hydrogen burning limit (Damiani et al. 2004; Prisinzano et al. 2005; Damiani et al. 2006; Prisinzano et al. 2007). With a nominal age of ∼1 Myr (e.g., Mayne et al. 2007), NGC 6530 is thus in many respects an analog of the ONC, but at a distance of ∼1.25 kpc NGC 6530 provides an ONC-like stellar laboratory beyond the immediate solar neighborhood.

An extensive literature has emerged over the past few years, characterizing the PMS population of NGC 6530 from X-ray to infrared wavelengths. Damiani et al. (2004) conducted the first large-scale study of the stellar population of NGC 6530. Using *Chandra* they detected 884 X-ray point sources, finding that 90%–95% of them constitute cluster members. Prisinzano et al. (2005) subsequently performed a complementary deep optical survey of the region, obtaining BVI_C photometry down to $V \approx 23$ using the Wide Field Imager at the MPG/ESO 2.2 m telescope. They matched their catalog to that of Damiani et al. (2004) and found 828 common stars, the vast majority of which are cluster members. From their deep color–magnitude diagrams (CMDs) and X-ray membership selection, they determined a cluster distance of 1.25 kpc and a modest cluster extinction of $A_V = 1.1$ mag, and they moreover estimated masses and ages for the stars through comparison with the PMS evolutionary tracks of Siess et al. (2000). Damiani et al. (2006) performed a near-infrared (NIR) survey of the cluster to identify stars with NIR excess emission indicative of objects bearing massive protoplanetary disks, and in the process increased the number of PMS cluster members to more than 1100. Prisinzano et al. (2007) spectroscopically studied a subsample of 332 cluster members, using Hα emission to classify the stars as classical T Tauri stars (CTTSs) or weak-lined T Tauri stars (WTTSs).

Our synoptic survey of the photometric variability properties of NGC 6530 builds on these studies. Our light curves of a $40' \times 40'$ region centered on NGC 6530 include the known cluster members as well as a total of ∼50,000 other stars within and surrounding the larger Lagoon Nebula star-forming region. These light curves in concert with the extant literature enable an array of variability studies for the region, including measurement of stellar rotation periods, identification of PMS eclipsing binaries, characterization of accretion-induced variations and stellar occultations due to disk obscuration, and discovery of eruptive variables. This first paper presents the results of our systematic search for rotation periods among the members of NGC 6530, the first such survey for stellar rotation periods yet reported for this important cluster.

Understanding the evolution of stellar angular momentum, particularly during the first few Myr of a star's life, remains one of the longest outstanding questions in star formation research (e.g., Vogel & Kuhi 1981; Hartmann et al. 1986; Bouvier et al. 1986). As PMS stars contract toward the main sequence, they would be expected to rapidly spin up to near breakup velocity as a consequence of angular momentum conservation. However, numerous surveys of rotation periods among low-mass PMS stars clearly show that these stars typically rotate at a small fraction of breakup, despite significant contraction in stellar radius (e.g., Stauffer & Hartmann 1987). A variety of mechanisms for efficiently removing angular momentum from PMS stars during the first ∼10 Myr has been proposed, including magnetic star–disk interaction (i.e., "disk-locking;" Koenigl 1991; Shu et al. 1994; Najita 1995; Ostriker & Shu 1995), scaled-up solar-type magnetized winds perhaps driven by accretion (e.g., Matt & Pudritz 2004, 2005a, 2005b, 2008a, 2008b), and scaled-up solar-type coronal mass ejections (e.g., Aarnio et al. 2009, 2010, 2011). However, the observational support for and theoretical efficacy of these mechanisms remains debated. There is not yet a consensus on the dominant mechanism(s) responsible for governing the angular momentum evolution of low-mass PMS stars.

In contrast, by the time a young cluster of stars reaches the age of the Pleiades (∼125 Myr), the observational picture is much more clear. By Pleiades' age, a cluster of coeval stars develops two distinct populations in period versus mass, now commonly referred to as the "I" and "C" sequences (Barnes 2003, 2007; Barnes & Kim 2010; Barnes 2010). These, respectively, correspond to curves that trace the upper and lower envelopes of stellar rotation periods. At an age of ∼600 Myr, about the age of the Hyades, nearly all stars inhabiting the "C" sequence will have spun down and transitioned onto the "I" sequence. This general behavior is attributed principally to changes in the stars' internal structures as a function of mass and has been found to hold true for clusters at a variety of ages (Patten & Simon 1996; Barnes et al. 1999; Allain et al. 1996; Krishnamurthi et al. 1998; Radick et al. 1987, 1990). While this "gyrochronology" paradigm has yet to be extended back to the PMS stage, it is clear that young low-mass stars must at some stage prior to the main sequence develop specific relationships between rotation period and stellar mass, and that these encode the stellar age. Exploiting the very young age of NGC 6530, we are in a position to better define the initial conditions of PMS angular momentum evolution, and to identify when and how the period–mass–age relationship begins to take shape.

In this paper, we report rotation periods for 290 members of NGC 6530. We match these to the literature to produce a catalog with which we investigate correlations between rotation period and other stellar properties, including disk presence, mass, age, spatial distribution within the cluster, and X-ray activity. In Section 2, we describe the photometric observations and their reduction, data from the literature, and the construction of our catalog. Our period search and statistical methods are discussed in Section 3. In Section 4, we examine the distribution of rotation periods, and investigate correlations between rotation period and the other stellar properties in our catalog. We discuss the implications of our results in Section 5, and in Section 6 we summarize the main conclusions.

Table 1
All Observational Data

Season	Telescope	Nights of Data
2004 Jun–Jul	CTIO 0.9 m	12
2005 Jul	CTIO 1.0 m	6
2006 Jun–Jul	CTIO 1.0 m	27
2007 Jun–Jul	CTIO 1.0 m	15
2008 Apr	CTIO 1.0 m	8
2009 May–Jun	CTIO 1.0 m	20

2. DATA

2.1. Observations

We have photometrically monitored the Lagoon Nebula over a period of several years using the SMARTS 1.0 m and 0.9 m telescopes at the Cerro Tololo Inter-American Observatory (CTIO). Table 1 summarizes the observing runs, the telescope used, and the number of nights with usable data for each.

Table 2
2006 Season Data

Field	α_{2000} (hh mm ss.s)	δ_{2000} (dd mm ss)	Exp. Time (s)	No. of Frames
1	18 05 01.6	−24 12 34	720	97
2	18 05 01.6	−24 29 34	720	95
3	18 03 46.9	−24 29 34	720	90
4	18 03 46.9	−24 12 34	720	85

For this paper we use the data from the longest of the observing runs, in 2006 June–July.

We repeatedly imaged the Lagoon Nebula on 27 clear nights over a time baseline spanning the 35 nights from June 15 to July 19. We used the Y4Kcam on the SMARTS 1.0 m telescope at CTIO. The observations consist of 720 s exposures taken through the Cousins *I* filter. The Y4Kcam has a field of view (FOV) of $20' \times 20'$ square, and we imaged four fields, alternating imaging each one. This gives us a full FOV of $40' \times 40'$ square which we imaged with a sampling cadence of $\sim$1 hr^{-1}. The field was centered on the NGC 6530 cluster, $(\alpha, \delta) = (18^{\rm h}04^{\rm m}24\overset{\rm s}{.}2, -24^\circ 21' 06\overset{''}{.}0)$ (J2000.0), the same as the *Chandra* observation of Damiani et al. (2004).

Table 2 gives an overview of the observations used in this paper. Figure 1 shows a 1×1 deg^2 image of the region with overlays of this study and the X-ray study of Damiani et al. (2004).

2.2. Data Reduction

The images were reduced, and instrumental magnitudes for all point sources extracted, using standard IRAF[5] procedures. Differential light curves were determined from point-spread function photometry using an algorithm for inhomogeneous ensemble photometry (Honeycutt 1992) as implemented in Stassun et al. (1999, 2002) for observations of high-nebulosity regions such as M8. We used a point-source detection threshold of 7σ above the sky background noise, and we kept only sources detected in at least 50 frames.

Figure 2 shows the rms of the light curves as a function of I_C magnitude (calibrated using the absolute photometry of Prisinzano et al. 2005) for each of the 53500 stars in our images. In the figure, the lower envelope of points with declining rms toward brighter I_C magnitude represents intrinsically non-variable stars to within the precision of our photometry, which is $\sim$0.008 mag at $I_C \approx 14$ and rising to $\sim$0.04 mag at $I_C \approx 18.0$ (the faint limit of our period search; see below). The rising envelope of rms for bright stars with $I_C \lesssim 14$ is due to CCD nonlinearity effects for stars approaching saturation ($I_C \approx 12.5$), and so we limit our period search to stars with $I_C \geqslant 13.0$ (see below).

We determined astrometric positions for each star in our catalog using the `astrometry.net` tool suite (Lang et al. 2010). The absolute positions of our sample stars are expected to be accurate to $\lesssim 1''$.

2.3. Data from the Literature

Large-scale X-ray observations of young clusters have demonstrated that X-ray emission is a highly efficient means for separating low-mass PMS stars from field contaminants (e.g., Getman et al. 2005a, 2005b; Güdel et al. 2007; Feigelson et al. 2011). For example, the *Chandra* Orion Ultradeep Project (COUP) found the rate of contaminants (due to foreground/background field stars and extragalactic sources) to be <10% (Getman et al. 2005a). Thus, we begin with the X-ray catalog of NGC 6530 from Damiani et al. (2004) to identify the most likely cluster members. They expect contamination in their population from non-member field stars to be $\sim$5%.

Table 3
X-Ray Positional Offsets

Field	ΔR.A.	ΔDecl.
1	$0\overset{''}{.}20$	$0\overset{''}{.}45$
2	$0\overset{''}{.}00$	$0\overset{''}{.}15$
3	$-0\overset{''}{.}30$	$-0\overset{''}{.}15$
4	$-1\overset{''}{.}05$	$-0\overset{''}{.}20$

First we match each of the stars in our photometric database to the Damiani et al. (2004) X-ray source list using a positional tolerance of $2''$. From this we determined the mean offsets between the two astrometric systems for each of our fields, which are listed in Table 3 (where offsets are positionally calculated as Damiani−ours), and corrected our astrometry to place all of the stars onto the Damiani et al. (2004) system. Then, we re-matched our stars to the Damiani et al. (2004) catalog employing a $1\overset{''}{.}5$ tolerance. This results in 662 unique cluster members which form the master sample for the present study. For these stars we also derive X-ray luminosities from the X-ray count rates reported by Damiani et al. (2004).

Stellar masses and ages come from the optical catalog of Prisinzano et al. (2005), and we use the isochrones of Siess et al. (2000) to infer stellar bolometric luminosities. We identify stars likely possessing warm, massive circumstellar disks using two different indicators—the reddening-free index of NIR excess, Q_{VIJK}, reported by Damiani et al. (2006), and the CTTS/WTTS classifications of Prisinzano et al. (2007) and Arias et al. (2007) based on their spectroscopic survey of Hα emitting stars in the cluster. Finally, known spectroscopic binaries are identified from the catalog of Prisinzano et al. (2007).

Figure 3 shows the V versus $V - I_C$ CMD for our X-ray-selected master study sample. The PMS evolutionary tracks of Siess et al. (2000) are overlaid for context (we transformed the tracks from effective temperature and bolometric luminosity to the CMD plane using the main-sequence relations of Kenyon & Hartmann 1995). The sample stars span a range of inferred masses $0.2 \lesssim M/M_\odot \lesssim 5$.

3. ANALYSIS

3.1. Period Search

We use the VARTOOLS light curve analysis program (Hartman et al. 2008) to search for periods in our light curves, employing the Lomb–Scargle (LS) period search algorithm (Lomb 1976; Scargle 1982; Press & Rybicki 1989; Press et al. 1992). Because the temporal baseline of our light curves is 35 days, we restrict the search to periods shorter than 20 days, i.e., just over 50% of the baseline. We also limit the search to periods longer than 0.1 days, corresponding to the Nyquist limit given our typical sampling frequency of $\approx$0.05 days (see Section 2). We first clipped the light curve data with iterative 3σ outlier rejection and then selected only those periods whose peaks in the resulting LS periodogram satisfied a signal-to-noise ratio (S/N) | S/N |> 4.0.

[5] IRAF is distributed by the National Optical Astronomy Observatory, which is operated by the Association of Universities for Research in Astronomy under cooperative agreement with the National Science Foundation.

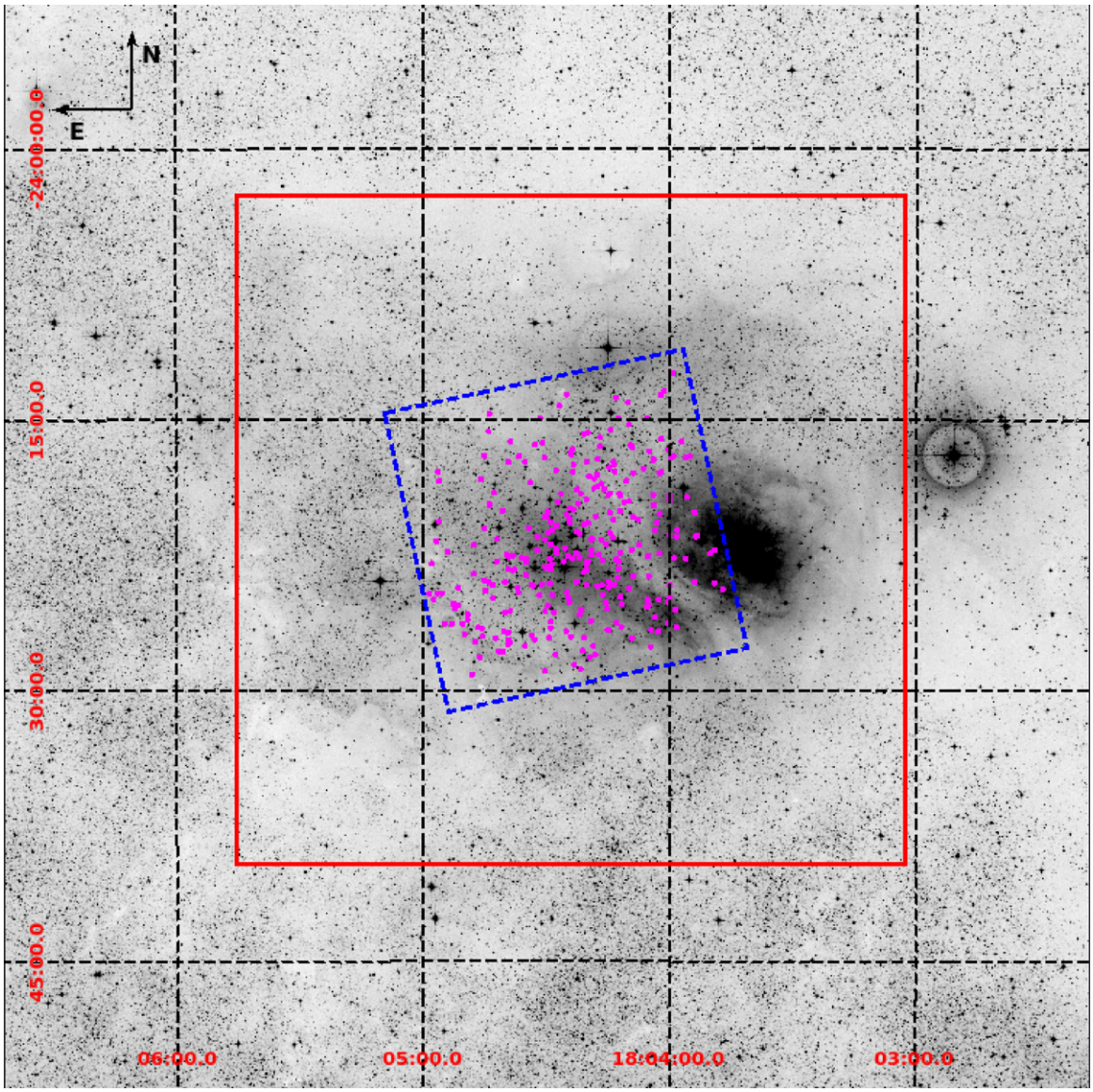

Figure 1. NASA SkyView image of the region around NGC 6530. The image size is 1×1 deg^2 and centered on $(\alpha, \delta) = (18^{\rm h}04^{\rm m}24\overset{\rm s}{.}4, -24^\circ 21' 06\overset{''}{.}0)$ with north up and east to the left. The area covered by this study is shown in red while the X-ray study of Damiani et al. (2004) is shown in dashed blue. Our 290 stars with rotation periods are shown in magenta.

(A color version of this figure is available in the online journal.)

We perform a Monte Carlo simulation with our observed light curves to determine the false-alarm probability (FAP) of the periods we detect. Following the procedures described in Stassun et al. (1999), for each star we generate 10,000 synthetic light curves from which we empirically determine the distribution of peak heights in the LS power spectrum that would arise from noise. We then compare the height of the peak in the star's observed LS power spectrum to this distribution of peak heights to determine the FAP. Each of the 10,000 synthetic light curves consists of two sources of noise. The first is the point-to-point scatter in the photometry which we simulate by scrambling the star's actual light curve data. The second is a correlated noise with a timescale of one day, whose amplitude we estimate from the standard deviation of nightly means from the star's light curve. The former preserves the specific noise distribution and the time sampling pattern of the actual data for each star, while the latter gives the synthetic light curves the freedom to vary on timescales that are long compared to our sampling interval, allowing them to mimic any slow variability of stellar origin (such as accretion activity) that could produce spurious periodic behavior that would be misinterpreted as a rotation period.

We consider "definite" rotation periods to be those with FAP $\leqslant 0.001$. In other words, these stars' LS power spectra evince peaks whose strengths occur by chance in 10 or fewer of the 10,000 noise light curves. As our master sample includes 662 stars, we therefore expect at most $\sim$1 false positive period. In addition, we consider "possible" rotation periods to be those with $0.001 < \mathrm{FAP} \leqslant 0.01$. Throughout our analysis we generally only utilize the definite rotation period stars, but we include the possible rotation period stars here for the benefit of future follow-up studies.

From our master sample of 662 cluster members, we find 256 definite periods and 47 possible periods. Finally, for the remainder of our analysis, we include only those stars included in the optical catalog of Prisinzano et al. (2005), for which

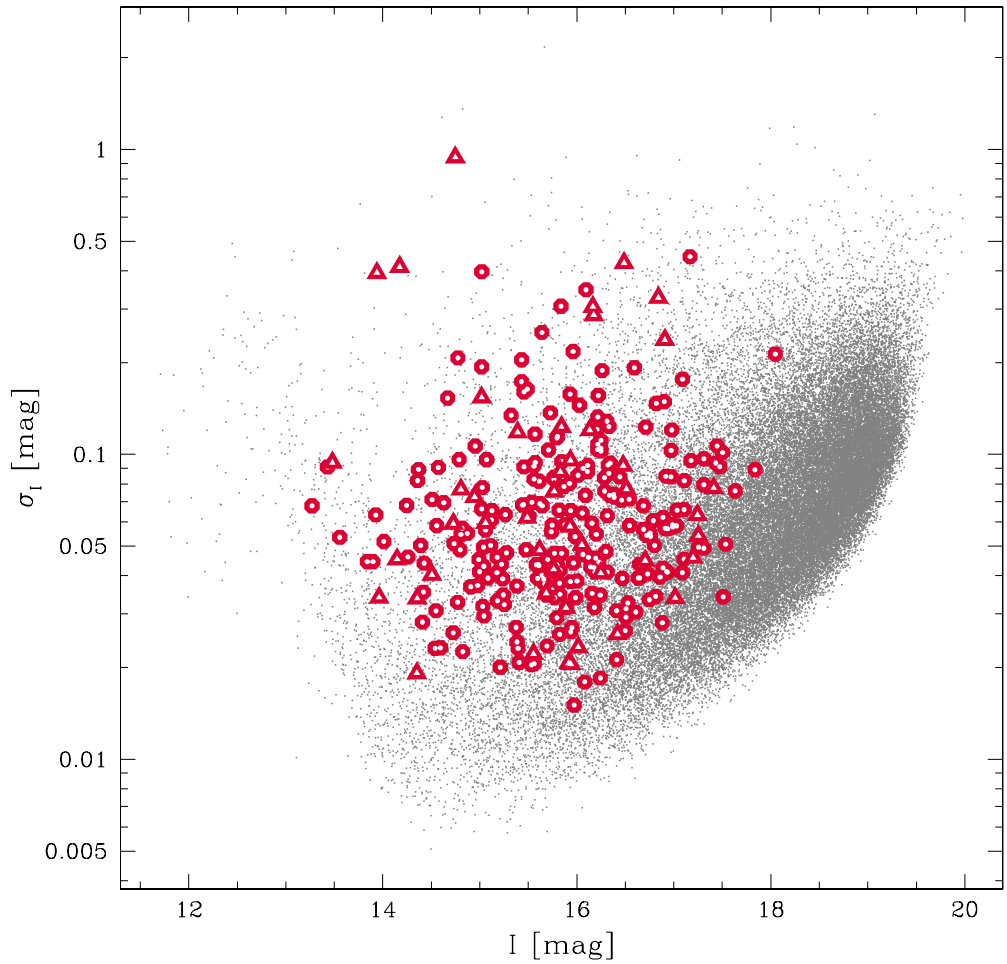

Figure 2. rms of the light curves as a function of calibrated I_C magnitude for the 53,500 stars in our four fields. The red circles denote the 244 stars with "definite" rotation periods (FAP $\leqslant 0.001$) while the red triangles mark the 46 stars with "possible" rotation periods ($0.001 <$ FAP $\leqslant 0.01$).
(A color version of this figure is available in the online journal.)

Table 4
Parameters of the 244 Cluster Members with Definite Rotation Periods

ID X-ray	ID WFI	R.A. (deg)	Decl. (deg)	V (mag)	I (mag)	Period (days)	Mass ($M_\odot$)	Age (Myr)	$L_{\rm bol}$ ($L_\odot$)	Radius ($R_\odot$)	$\log(L_{\rm X})$ (erg s^{-1})	IR excess?	Hα class?[a]	SB2?
423	14403	271.09209	−24.42964	15.692	13.557	0.10352	0.69	0.35	5.12	4.49	29.382	N	···	N
138	27470	271.02700	−24.29480	17.948	16.261	0.18743	0.94	22.23	0.39	0.96	29.566	···	···	N
067	28743	270.99692	−24.28292	19.389	16.527	0.24286	0.36	2.02	0.32	1.44	29.331	···	···	···
024	21464	270.97288	−24.35667	14.522	13.271	0.49948	1.85	6.22	7.02	2.61	30.815	N	W	N
040	25374	270.98342	−24.32083	18.483	16.215	0.65205	0.57	3.00	0.43	1.37	29.895	···	···	···

Notes.
[a] C denotes Classical T Tauri stars while W identifies Weak-lined T Tauri stars.
[b] These Hα classifications are taken from Arias et al. (2007); all others come from Prisinzano et al. (2007).

(This table is available in its entirety in a machine-readable form in the online journal. A portion is shown here for guidance regarding its form and content.)

we have estimated stellar masses and ages. This yields a final catalog of 244 cluster members with definite periods and 46 with possible periods. The sample of 244 definite periods represents the successful detection of periods for one-third of the Damiani et al. (2004) X-ray catalog of NGC 6530 cluster members. The full catalogs of cluster members with definite and possible rotation periods are in Tables 4 and 5, respectively, along with all of the associated data that we have gleaned from the literature (see Section 2.3). Figure 4 shows the phase-folded light curves of the 244 definite rotators, ordered by increasing period. Figure 5 shows the same for the 46 possible rotators.

The definite and possible rotators are also highlighted in the CMD shown in Figure 3. Our sample of rotators span the range $13.0 \lesssim I_C \lesssim 18.0$. Note that many stars with high rms are not identified here as rotation period detections because they were not identified as cluster members in the X-ray study of Damiani et al. (2004); future investigations of cluster membership would enable an even larger sample of rotation period determinations for NGC 6530 from our light curves.

We quantify our period detection sensitivity and any biases as functions of period and stellar brightness. We use 1000 of the non-variable stars in our full data set, and that are in the

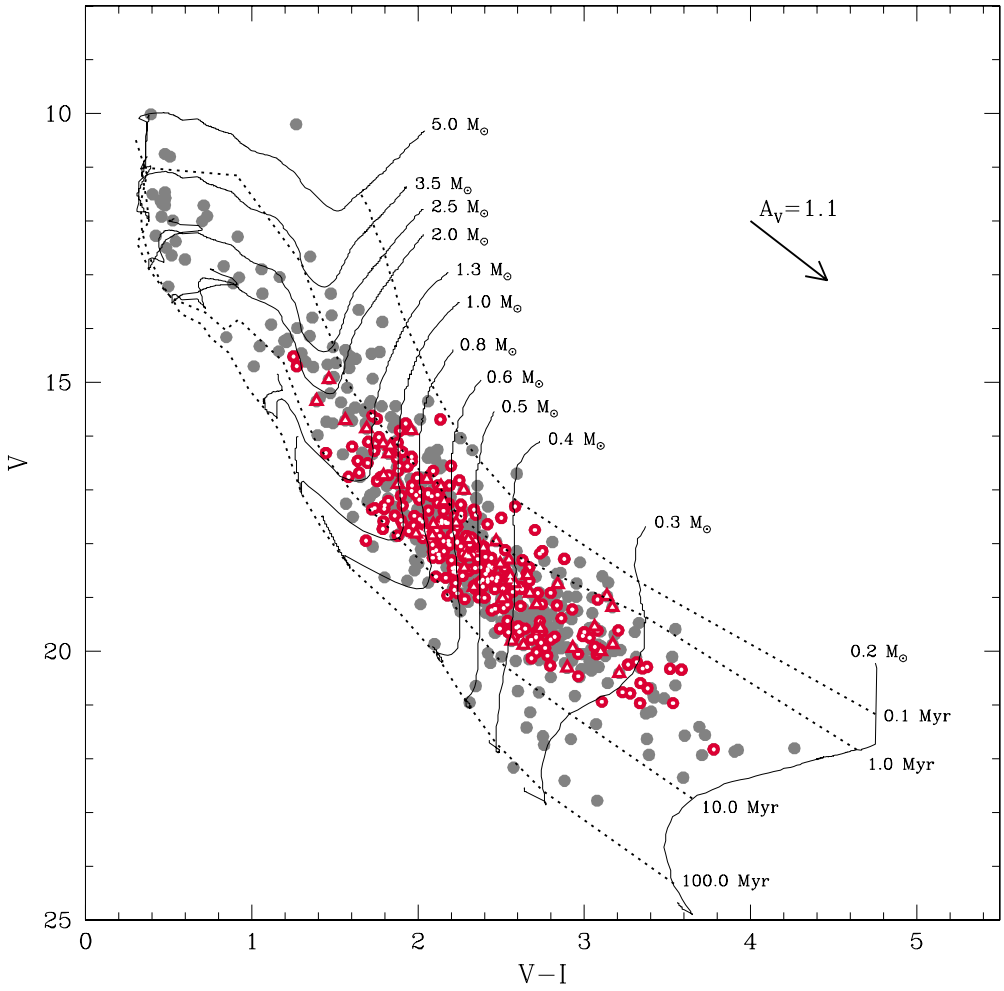

Figure 3. V vs. $V - I_C$ color–magnitude diagram for our master sample drawn from the catalog of X-ray members of Damiani et al. (2004; filled symbols). Stars for which we report rotation periods are highlighted. Overplotted are the PMS evolutionary tracks of Siess et al. (2000) assuming a distance of 1.25 kpc and an extinction of $A_V = 1.1$ mag (Prisinzano et al. 2005). The reddening vector shown uses the above A_V and the color excess $E(V - I) = 0.46$ value from Prisinzano et al. (2005). (A color version of this figure is available in the online journal.)

Table 5
Parameters of the 46 Cluster Members with Possible Rotation Periods

ID X-ray	ID WFI	R.A. (deg)	Decl. (deg)	V (mag)	I (mag)	Period (days)	Mass ($M_\odot$)	Age (Myr)	L_{bol} ($L_\odot$)	Radius ($R_\odot$)	log(L_X) (erg s^{-1})	IR excess?	Hα class?[a]	SB2?
217	25571	271.05200	−24.31766	17.959	15.489	0.3999630	0.45	1.01	0.84	2.12	29.890	...	...	...
425	21654	271.09217	−24.35480	17.818	15.830	0.6353953	0.88	5.26	0.56	1.34	29.822	...	...	...
581	13973	271.12150	−24.43629	19.875	16.704	0.6393026	0.32	1.95	0.30	1.45	29.406	...	...	...
126	15028	271.02154	−24.42041	19.131	16.418	0.6978532	0.38	1.57	0.44	1.64	29.490	...	...	...
732	28075	271.16463	−24.28881	17.645	15.552	0.7891157	0.73	2.56	0.73	1.64	29.601	Y	W	N

Notes.
[a] C denotes Classical T Tauri stars while W identifies Weak-lined T Tauri stars.
[b] These Hα classifications are taken from Arias et al. (2007); all others come from Prisinzano et al. (2007).

(This table is available in its entirety in a machine-readable form in the online journal. A portion is shown here for guidance regarding its form and content.)

same magnitude range as our rotators, as a control sample. For each star we inject sinusoids with amplitude in the range $0.02 \leqslant \Delta I \leqslant 0.2$, typical for our sample of rotators (see Figure 4), into the light curves with periods in the range 0.1–20 days and run the VARTOOLS LS period search algorithm using the same criteria as above. We consider the period successfully recovered if it agrees with the input period to within 10%, which is an acceptable margin of error in the rotation periods for the purposes of our analysis below. Some of the observed light curves for our sample of rotators show modest departures from sinusoidal shapes (see Figure 4), but we expect any resultant errors in the periods to be within the 10% tolerance that we adopt for this test.

Figure 6(a) shows the fraction of correctly recovered periods as a function of input period, while Figure 6(b) shows the fraction of correctly recovered periods as a function of I_C magnitude. We find that our period detection efficiency is roughly constant at ≈90% for the full range of rotation

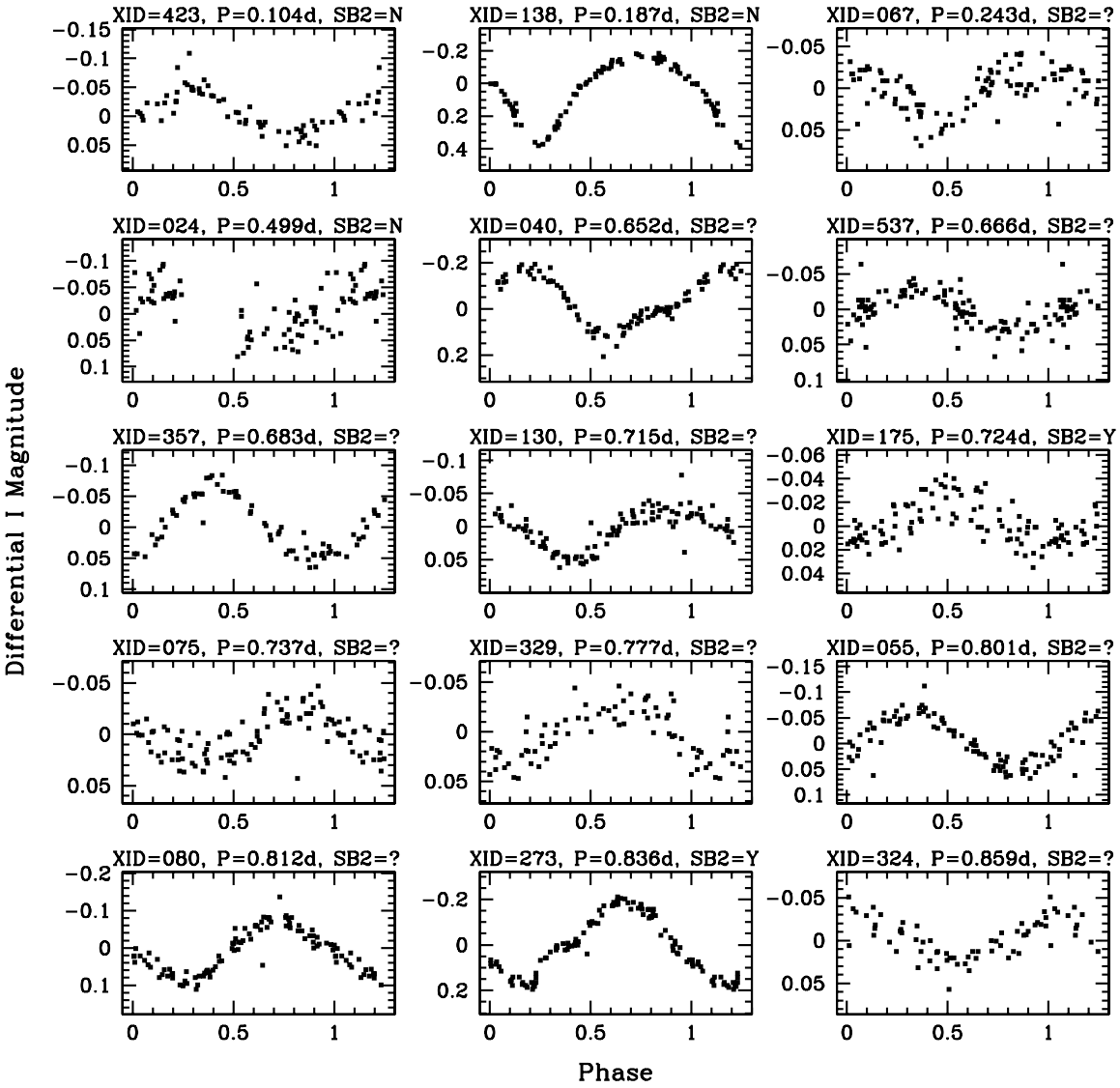

Figure 4. Light curves of NGC 6530 cluster members with "definite" rotation periods (FAP $\leqslant 0.001$). The light curves are folded on the derived rotation period (shown above each light curve) and replicated over an additional 0.25 phase for clarity. Also shown above each light curve is the ID number from the X-ray study of Damiani et al. (2004), as well as a flag indicating whether previous spectroscopic observations suggest the star is a spectroscopic binary (SB2). The stars are shown ordered by increasing period.

(An extended version of this figure is available in the online journal.)

periods tested. Thus, while this simulation suggests we are missing ∼10% of the true underlying population of rotators, with variability amplitudes larger than 0.02 mag, we infer no strong biases in the rotation period distribution as a function of period. At the same time, there is a strong bias against period detection for the bright stars with $I_C \lesssim 14$, clearly the result of the higher rms in our light curves for the brightest stars (see Section 2.1). For fainter stars the detection efficiency is approximately 100%, and thus the ∼10% loss of efficiency seen in Figure 6(a) is entirely a consequence of the brighter stars. However, again, Figure 6(a) indicates that this loss of efficiency is largely independent of period, and thus we expect no strong biases in the period distribution of our sample. Figure 6(c) shows that our detection efficiency is also independent of amplitude over this range. We also performed a simulation with injected amplitudes as low as 0.002 mag and found that our sensitivity remained high down to $\Delta I \sim 0.006$ mag. However, given the simple nature of these simulations (e.g., we inject perfectly sinusoidal signals), we conservatively assume that we are not sensitive to periodic variations below ∼0.02 mag given the ∼0.01 mag precision in the photometry.

Finally, we note that 21 of the 244 stars in the definite rotator group have been previously identified as candidate spectroscopic binaries (SB2s; see Table 4). In these cases it is possible that the periodicity we observe is related to the binary orbit but not to the rotation of the star(s), or that the rotation of the star dominating the light has been affected by the presence of a close faint companion star. We do not attempt to correct for these possibilities, but note here that these SB2s constitute less than 10% of our sample and are not concentrated at specific rotation periods, so we do not expect these to alter our results. We do comment on specific interesting cases below. We note that those SB2s with shorter periods could potentially be non-member field contaminants. Our catalog of members with rotation periods is X-ray-selected, and tidally locked short-period binaries in the foreground might display enhanced X-ray emission that would mimic that of cluster members.

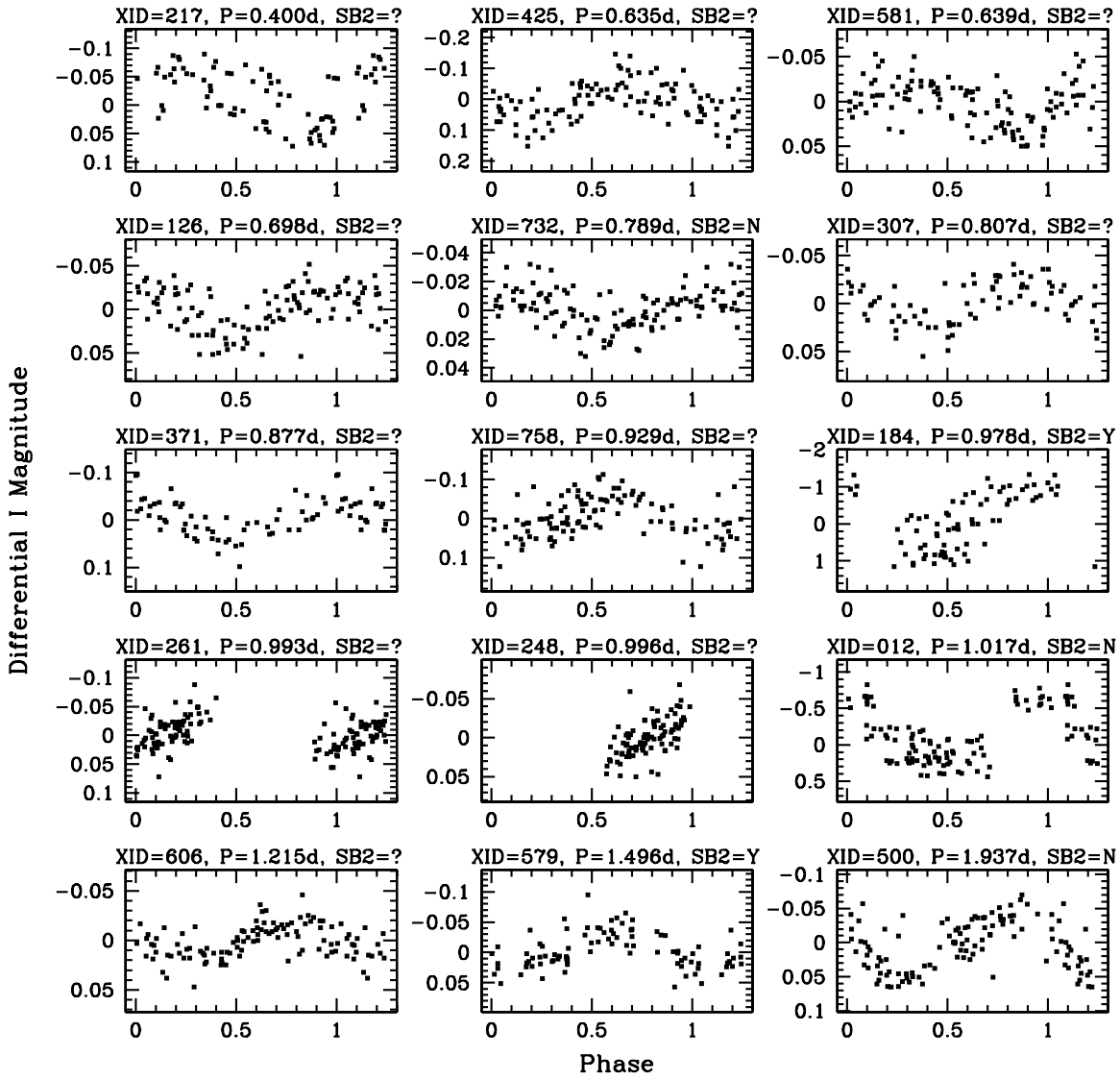

Figure 5. Same as Figure 4 but for NGC 6530 cluster members with "possible" rotation periods ($0.001 < \mathrm{FAP} \leqslant 0.01$).
(An extended version of this figure is available in the online journal.)

3.2. Correlation Tests

We employ two standard statistical tests to examine possible differences or trends in the rotation periods as a function of various stellar properties: the Kolmogorov–Smirnov (K-S) test, which determines the probability that two samples were drawn from the same parent distribution, and the Student's *t*-test, which determines the probability that two samples possess identical means. For a given stellar property (e.g., mass), we divide the period distribution into two bins (e.g., low mass and high mass) and apply these statistical tests on the rotation periods of the two bins. In all of the statistical comparisons below we include only stars with definite rotation periods as defined above (see Section 3.1).

4. RESULTS

4.1. Period Distribution

Figure 7 shows the rotation period distribution of our entire sample of 244 cluster members with definite periods. The masses and ages for these stars from Prisinzano et al. (2005) using the PMS evolutionary tracks of Siess et al. (2000) are shown in Figure 8. The typical star in our sample is inferred to have $M_\star \sim 0.6\,M_\odot$ and age ~2 Myr according to these tracks (but see Section 5 for a detailed discussion of the likely age of the cluster). Correlations between the rotation periods and these masses and ages are discussed below.

The distribution is roughly flat for $P \leqslant 10$ days. A peak is apparent near $P = 1$ day, which may suggest that some aliasing effects at the diurnal sampling frequency of the light curves are still present. Despite this, a one-sided K-S test comparing the observed distribution with a uniform distribution for $P \leqslant 10$ days yields a probability of 18% that the two distributions represent the same parent population. Thus, the null hypothesis—a uniform distribution in this case—is not rejected by the observed period distribution.

We observe two clear cutoffs in the period distribution, despite our good sensitivity to periodic signals for periods both longer and shorter than the observed cutoffs. At the long period end, the distribution tapers off strongly for $P \gtrsim 10$ days. This is very similar to the observed long-period cutoff in the distributions of other young clusters, such as the ONC (e.g., Stassun et al. 1999).

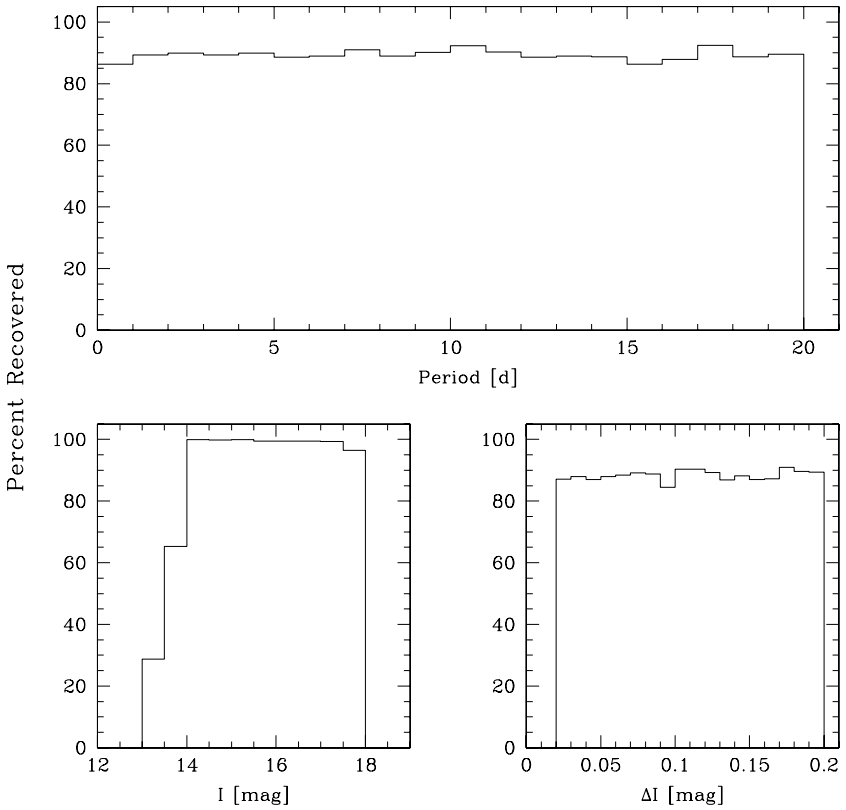

Figure 6. Efficiency of period detection. Top: this figure shows the fraction of correctly detected periods as a function of input period, using as a control our light curves of non-variable stars spanning the same range of I_C magnitudes as our sample of rotators. We inject sinusoids with amplitudes in the range $0.02 \leqslant \Delta I \leqslant 0.2$ mag into the light curves, and consider the period successfully recovered if it matches the input period to within 10%. Bottom left: same as the top panel, but showing the period recovery fraction as a function of I_C magnitude. Bottom right: same as other panels, but showing the period recovery fraction as a function of injected amplitude.

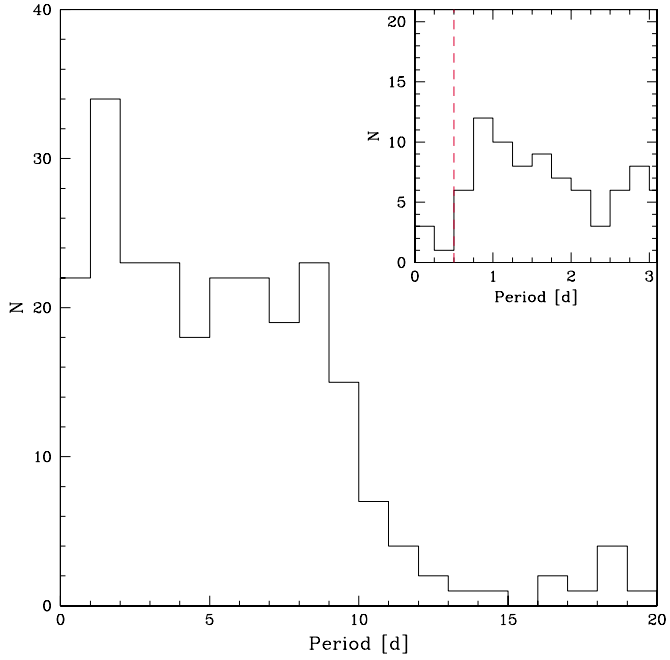

Figure 7. Period distribution of our sample of 244 definite NGC 6530 rotators, with bins of one day. The inset shows the same distribution, but with 0.25 day bins at the short-period end of the distribution. The vertical line in the inset shows approximately the rotation period corresponding to breakup speed for the typical rotator in our sample.

(A color version of this figure is available in the online journal.)

At the short-period end, the distribution drops dramatically for $P \lesssim 0.5$ days. For the typical star in our sample, with $M_\star \approx 0.6\,M_\odot$ and $R_\star \approx 2.2\,R_\odot$ (according to the PMS tracks of Siess et al. 2000), the rotation period corresponding to breakup velocity is ≈0.5 days. Therefore, we ascribe the short-period cutoff to a real physical limit on the minimum rotation period for the stars in our sample.

4.2. Disk and Accretion Indicators

We use the reddening-free index of NIR excess, Q_{VIJK} (Damiani et al. 2006), to segregate our sample according to the likelihood that they possess massive circumstellar disks. Those stars that are identified in Damiani et al. (2006) as having a high Q_{VIJK} value display significant IR emission relative to their optical color, and we adopt their same classifications to indicate which stars harbor a circumstellar disk. We note that Q_{VIJK} is a fairly crude measure of NIR excess, and certainly does not yield information on disk structure. Stars without large Q_{VIJK} index values may still possess disks, for example, if the disk has an evacuated inner hole. We perform a two-sided K-S test as well as a *t*-test to compare the period distributions of the "disked" and "non-disked" stars. Table 6 gives the number of stars in each group and the details of the statistical results. We find that the period distribution for stars with NIR excess is statistically different from those without NIR excess, with a ∼1% probability that they were drawn from the same distribution. We also find that the means of the distributions (6.3 and 3.7 days for the disked and non-disked stars, respectively) have only a ∼0.1% probability of being the same (i.e., the difference in means is statistically significant). Figure 9(a) offers a visual

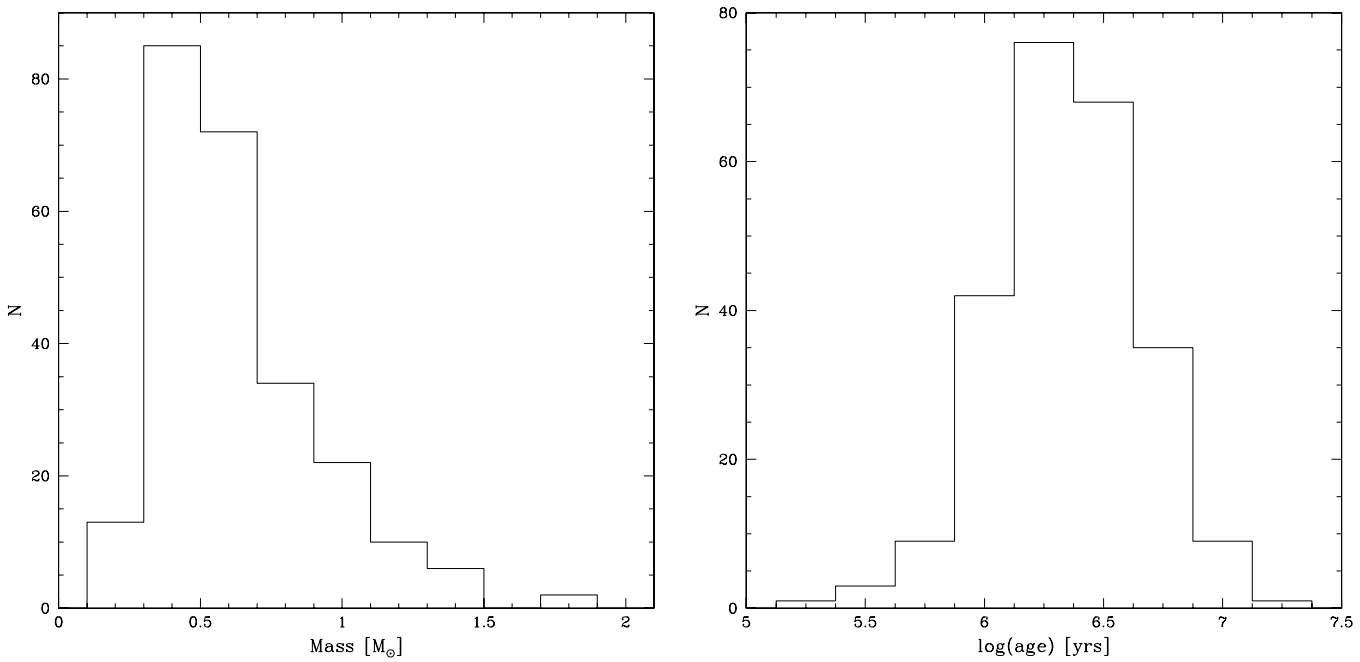

Figure 8. Distributions of masses (left) and ages (right) for our sample of NGC 6530 cluster members with rotation periods (see Figure 7). Masses and ages are inferred from the PMS evolutionary tracks of Siess et al. (2000).

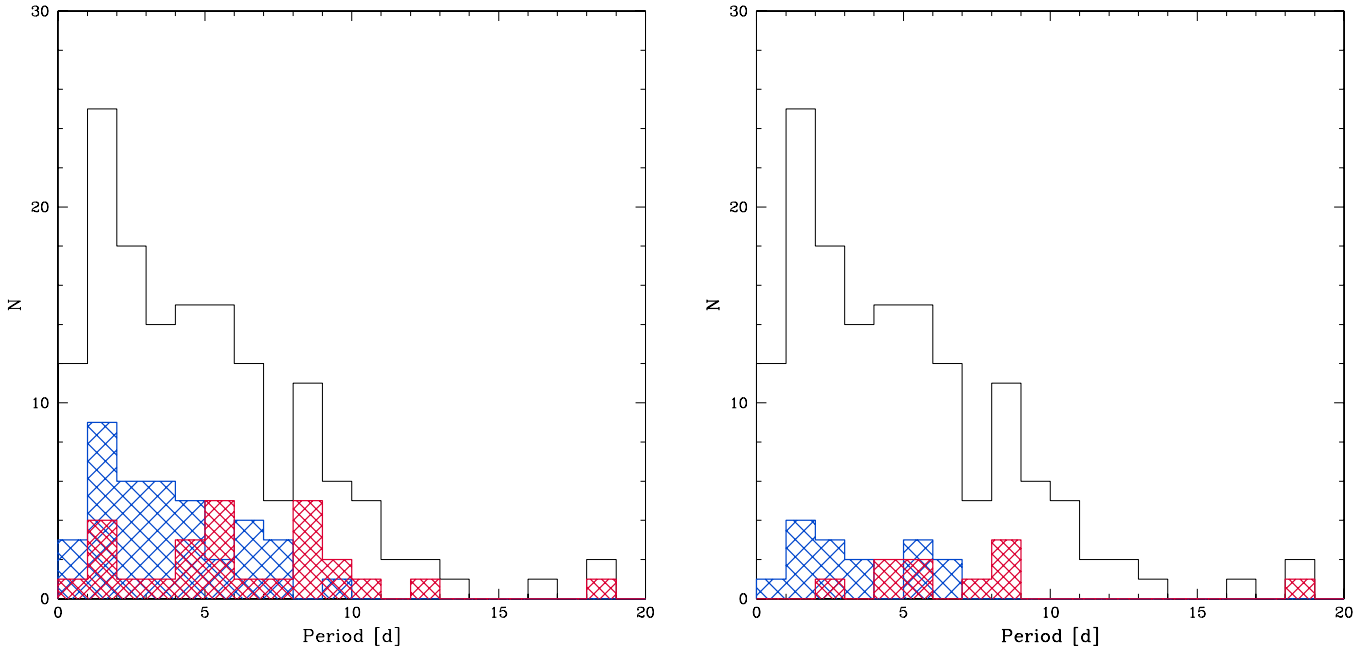

Figure 9. Left: rotation period distributions of NGC 6530 cluster members exhibiting NIR excess emission indicative of disks (shaded red histogram) and those that do not exhibit NIR excess emission (hatched blue histogram), as determined via the Q_{VIJK} index (Damiani et al. 2006). A K-S test and a Student's *t*-test both indicate that distributions of NIR excess stars vs. non-excess stars are statistically different, with the NIR excess stars rotating more slowly on average (see Table 6). Right: rotation period distributions of NGC 6530 cluster members classified as CTTSs (red) and WTTSs (blue) based on strength of Hα emission (Prisinzano et al. 2007; Arias et al. 2007). A K-S test and a Student's *t*-test both indicate that distributions of CTTSs vs. WTTSs are statistically different, with the CTTSs rotating more slowly on average (see Table 6). In both panels the open (black) histogram shows the rotation period distribution for the entire sample (see Figure 7), but including only "high-mass" stars with $M_\star > 0.5 M_\odot$ because the NIR excess and T Tauri star samples are observationally biased against low masses (see the text).

(A color version of this figure is available in the online journal.)

comparison of this result. While those stars with no NIR excess are concentrated at faster periods, those with NIR excess are more uniformly distributed and exhibit a significant long-period component.

We also segregate the sample into accretors and non-accretors based on their classification as a CTTS or WTTS, as determined from their Hα emission strength. The distributions are shown in Figure 9(b). The number of classified CTTS and WTTS stars is small; however, the WTTSs appear to be concentrated at faster rotation periods while the distribution for CTTSs is shifted toward longer periods. To quantify the comparison we again perform a two-sided K-S tests as well as a *t*-test. The sample sizes and statistical results are in Table 6. The probability that the two-period distributions were drawn from the same

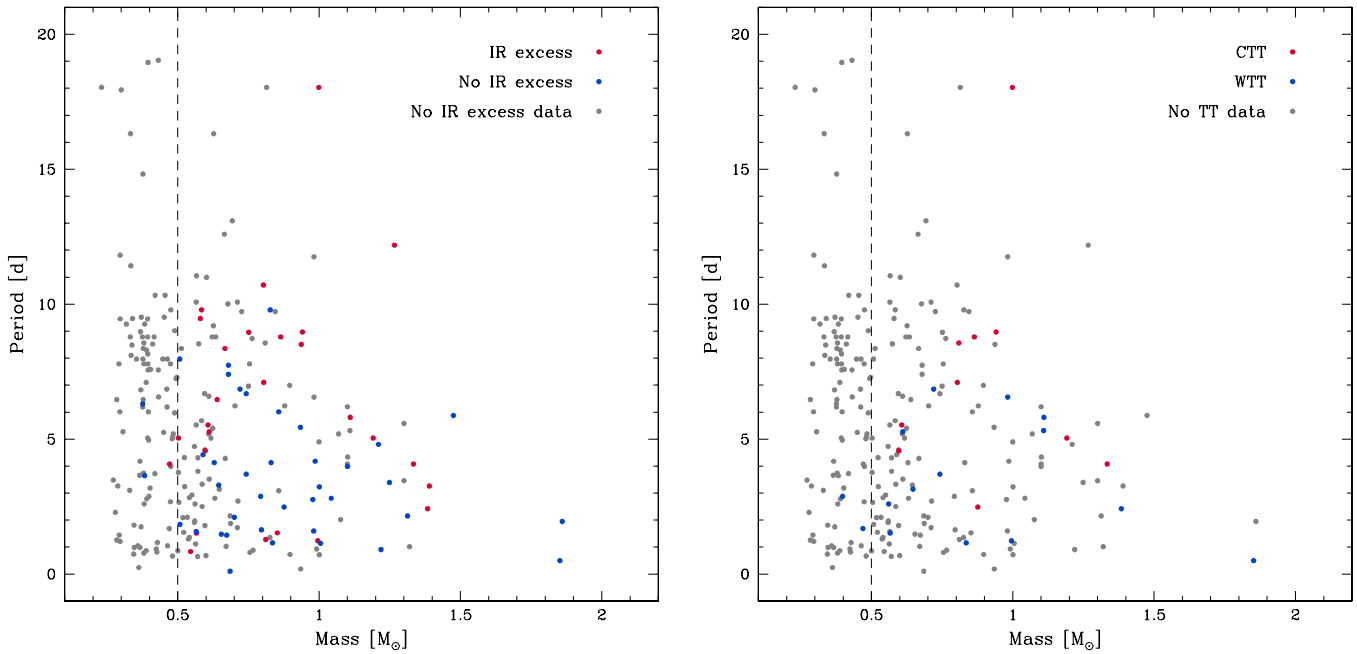

Figure 10. Period vs. mass for our sample of NGC 6530 rotators. Left: red points are those stars identified as having NIR excess as measured via the Q_{VIJK} index (Damiani et al. 2006), blue points are those with no NIR excess, and gray points are the remainder of the sample (no NIR classification). Right: red points are those stars identified as CTTSs, blue points are WTTSs (Prisinzano et al. 2007; Arias et al. 2007), and gray points are the remainder of the sample (no Hα spectrum available). In both panels, the dashed vertical line demarcates the two mass bins we use for statistically comparing the period distribution as a function of stellar mass. A K-S test and a Student's *t*-test both reveal a statistically significant tendency for the lower mass stars to rotate more slowly on average than the higher mass stars (see Table 6).
(A color version of this figure is available in the online journal.)

Table 6
Statistical Comparisons of Rotation Periods

	N	$\langle P \rangle$	K-S Prob.	t Prob.
NIR excess	27	6.253		
No NIR excess	39	3.679	0.0125	0.00160
CTT	10	7.316		
WTT	15	3.376	0.0248	0.00590
Low mass	98	6.357		
High mass	146	4.929	0.00104	0.00511
Young	92	4.890		
Old	152	5.873	0.0136	0.0575
Northwest	79	5.199		
Southeast	70	6.238	0.0115	0.117
Northeast	30	5.982		
Southwest	65	4.858	0.141	0.175

parent distribution is only ∼2%, and the probability that their means (7.3 and 3.4 days for the CTTS and WTTS samples, respectively) are identical is only 0.6%.

4.3. Stellar Mass

Figure 10 shows rotation period as a function of stellar mass (inferred from the PMS evolutionary tracks of Siess et al. 2000) for the sample of NGC 6530 rotators. There is an apparent trend of decreasing rotation period (faster rotation) toward the higher stellar masses. We also show in the figure the stars for which we have NIR excess information (left panel) and the stars for which we have CTTS/WTTS status information (right panel). There is a clear bias present such that almost none of the stars with either NIR excess information or CTTS/WTTS status are present for $M_\star < 0.5\,M_\odot$. This is the result of the observational limits of the NIR and spectroscopic surveys of the cluster, which were not sensitive to the fainter, low-mass members of the cluster (Prisinzano et al. 2007; Arias et al. 2007).

As an initial quantitative measure of the dependence of rotation period on stellar mass, we divide the sample of rotators into two groups of comparable size based on the overall distribution of the stellar masses (see Figure 8): a "low-mass" group with $M_\star \leqslant 0.5\,M_\odot$, and a "high-mass" group with $M_\star > 0.5\,M_\odot$. We chose the mass cut to be at 0.5 $M_\odot$ because previous studies have suggested a change in the behavior of the period distribution at around 0.4 $M_\odot$ (for the Siess et al. 2000 tracks used here), but dividing the sample at 0.4 $M_\odot$ would have created imbalanced groups (63 "low-mass" stars to 181 "high-mass" stars) for definite rotators in our catalog. We have checked that all statistical results reported below based on this mass division are not changed qualitatively if we instead cut on 0.4 $M_\odot$. Figure 11 compares the period distributions of these two mass groupings, which are clearly different. A K-S test gives that the probability of the two period distributions being drawn from the same parent distribution is only 0.1%, and a *t*-test gives a probability of only 0.5% that the means of the two period distributions are identical (see Table 6). The high-mass stars rotate faster than the low-mass stars; their mean rotation periods are 4.9 and 6.4 days, respectively (Table 6).

4.4. Stellar Age

Figure 12 shows rotation period as a function of age (inferred from the isochrones of Siess et al. 2000) for our sample of NGC 6530 rotators. Here any trends between the rotation periods of the stars and their inferred ages are more subtle than is the case with stellar mass (see above). The stars with available NIR excess and CTTS/WTTS status indicators are not strongly biased with respect to inferred stellar age.

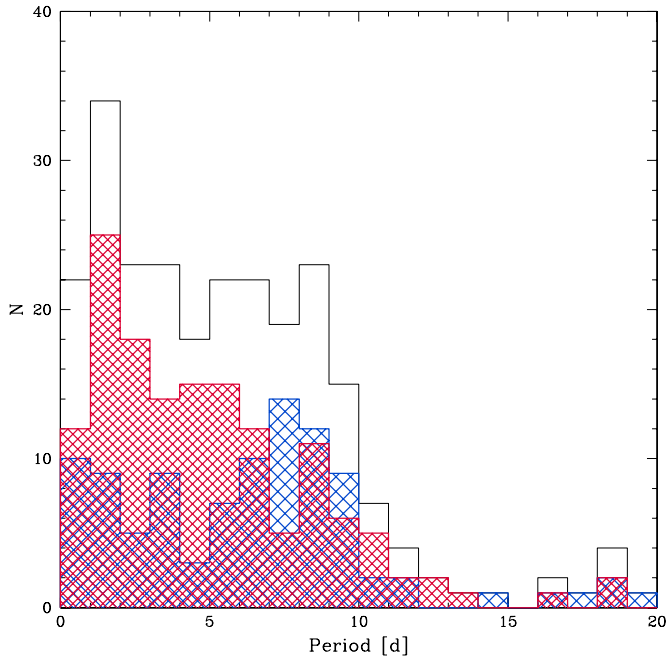

Figure 11. Comparison of the rotation period distributions for "high-mass" and "low-mass" stars in our sample of NGC 6530 rotators. The red shaded histogram represents stars with $M_\star > 0.5\,M_\odot$ and the blue hatched histogram represents stars $M_\star \leqslant 0.5\,M_\odot$. A K-S test and a Student's t-test both indicate strong statistical differences between the rotation periods of the high-mass and low-mass stars, with the high-mass stars rotating faster on average (see Table 6).

(A color version of this figure is available in the online journal.)

To quantify any relationship between rotation period and inferred stellar age, we divide the sample into two age groups. Based on the distribution of inferred stellar ages (see Figure 8(b)), we divide the stars into a "young" group with log(age/yr) $\leqslant$ 6.25 and an "old" group with log(age/yr) $>$ 6.25. As was suggested visually in Figure 12, a t-test does not indicate strong evidence for a statistically significant difference in the mean periods of the two groups (Table 6). However, a K-S test does indicate that the young and old stars have only a 1.4% chance of being drawn from the same parent rotation period distribution. We conclude that there is weak evidence for a difference in the rotation period distributions of the stars as a function of inferred stellar age, with the older stars rotating slightly more slowly on average (mean rotation periods 5.9 and 4.9 days, respectively; Table 6).

4.5. Spatial Distribution

Previous works have suggested evidence for sequential star formation in NGC 6530 and the larger Lagoon Nebula region. For example, Lada et al. (1976) suggested that star formation has progressed from NGC 6530 to Herschel 36, nearby and to the west. Similarly, the X-ray study of Damiani et al. (2004) found evidence for an age gradient in NGC 6530, wherein the younger stars are more concentrated in the southeast and older stars in the northwest (cf. Figure 12 in that paper).

Figure 13 shows the spatial distribution of our sample of rotators in NGC 6530. Following Damiani et al. (2004) we divide the cluster into quadrants (northwest, southeast, etc.) and perform our statistical tests on the rotation period distributions of the stars in different pairs of quadrants. As shown in Table 6, the Student's t-test does not indicate any statistically significant difference in the mean rotation periods as a function of spatial position. However, a K-S test does show a modestly significant difference in the period distributions when the southeast quadrant is compared to the northwest quadrant, with a probability of $\sim$1% that the rotation period distributions of the two groups were drawn from the same parent distribution. The mean rotation periods in the southeast and northwest quadrants

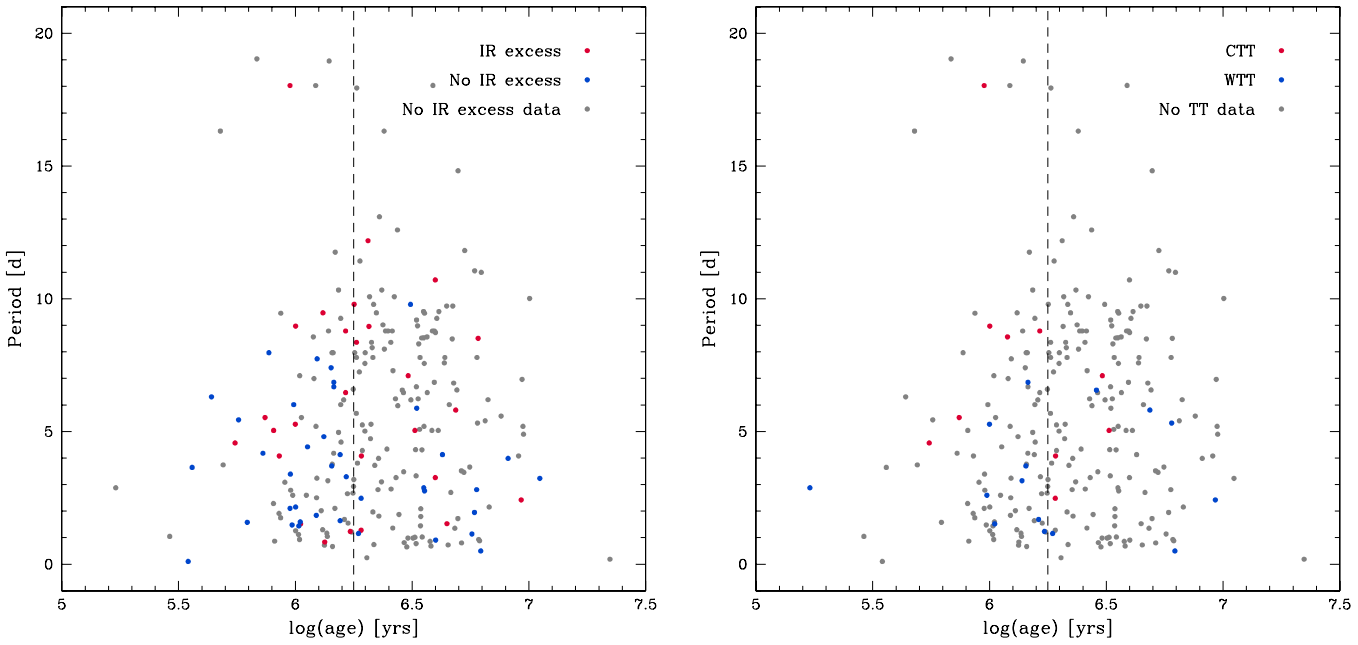

Figure 12. Period vs. age for our sample of NGC 6530 rotators. Left: red points are those stars identified as having NIR excess as measured via the Q_{VIJK} index (Damiani et al. 2006), blue points are those with no NIR excess, and gray points are those with no NIR classification. Right: red points are those stars identified as CTTSs, blue points are WTTSs (Prisinzano et al. 2007; Arias et al. 2007), and gray points are those with no Hα spectrum. In both panels, the dashed vertical line demarcates the two age bins used in our comparison of "old" vs. "young" stars. A K-S test suggests a mild tendency for the younger stars to rotate more rapidly on average (see Table 6).

(A color version of this figure is available in the online journal.)

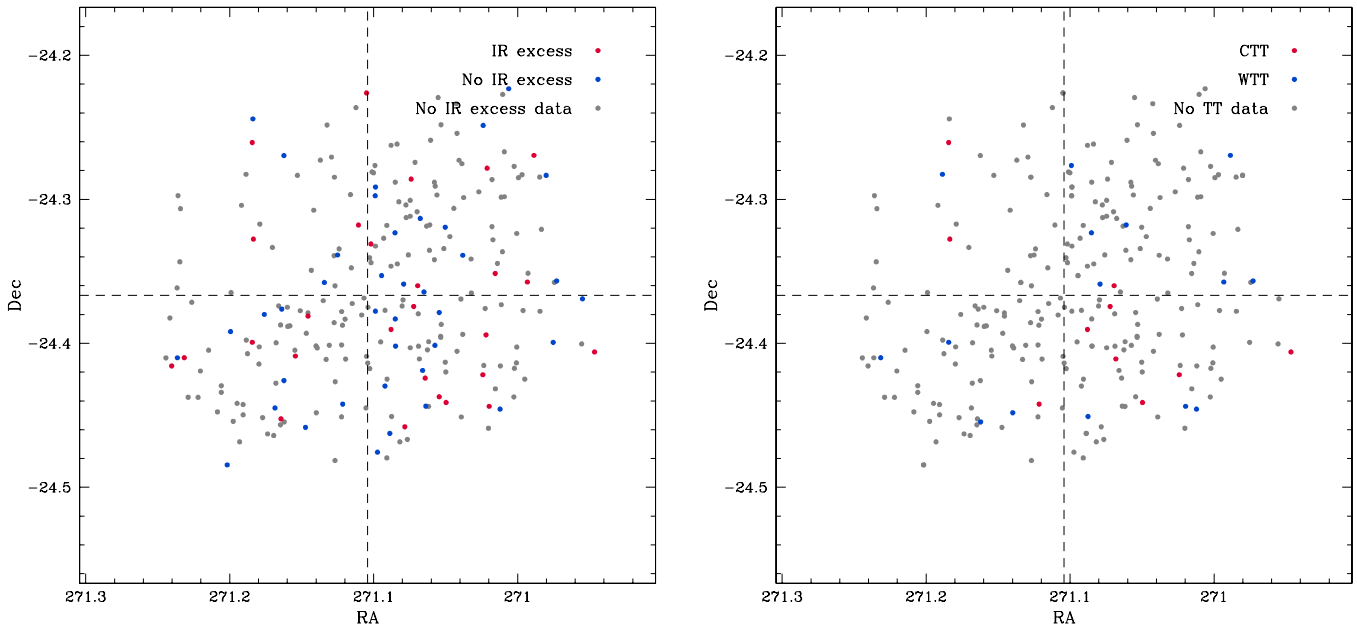

Figure 13. Spatial distribution of our sample of NGC 6530 rotators. Left: red points are those stars identified as having NIR excess in the Q_{VIJK} index (Damiani et al. 2006), blue points are those with no NIR excess, and gray points are those with no NIR classification. Right: red points are those stars identified as CTTSs, blue points are WTTSs (Prisinzano et al. 2007; Arias et al. 2007), and gray points are those with no Hα spectrum. In both panels, the dashed lines demarcate the quadrants that we use to investigate gradients in age and rotation within the cluster (see also Damiani et al. 2004). A K-S test suggests a potential southeast–northwest gradient in the rotation periods.

(A color version of this figure is available in the online journal.)

are 6.2 and 5.2 days, respectively (Table 6). Together with the age gradient found above, this difference in periods would imply that the younger stars (to the southeast) rotate more slowly on average than the older stars (to the northwest).

However, this is in the opposite sense of the (weak) period–age trend found above, in which the isochronally younger stars rotate more rapidly on average. Thus, we conclude that any trends in rotation with isochronal age or with age inferred from spatial location are weak at best and inconsistent in sense.

4.6. X-Ray Activity

To investigate the relationship between the rotation period of NGC 6530 cluster members and their X-ray activity, we require estimates of the X-ray luminosities (L_X) and the bolometric luminosities ($L_{\rm bol}$) of the stars in our sample. Neither of these quantities was tabulated by the previous studies of the cluster, so here we adopt a procedure to provide estimates of both quantities.

To estimate L_X for each star, we use the PIMMS software[6] to convert the X-ray count rates of Damiani et al. (2004) into X-ray fluxes, using the PIMMS MEKAL model. The model requires as input the temperature of the emitting coronal gas (kT) and the hydrogen column density toward the source. For kT, we adopt the median of the kT distribution found by COUP (Getman et al. 2005b). We adopt an extinction of $A_V = 1.1$ to the cluster (Prisinzano et al. 2005), which yields a hydrogen column density of $N_{\rm H} = 2.431 \times 10^{21}$ cm^{-2} (Güver & Özel 2009). Finally, adopting a cluster distance of 1.25 kpc (Prisinzano et al. 2005), we convert the PIMMS X-ray fluxes into L_X. This approach obviously does not take into account potential differences in kT or A_V to individual stars; however, as only the X-ray count rates are available from Damiani et al. (2004), a more sophisticated approach is not warranted.

[6] Distributed by NASA's High Energy Astrophysics Science Research Center; http://heasarc.gsfc.nasa.gov/docs/software/tools/pimms.html.

Table 7
Statistical Comparisons of X-Ray Luminosities

	N	$\langle\log(L_X/L_{\rm bol})\rangle$	K-S Prob.	t Prob.
Fast	79	−3.556		
Slow	165	−3.372	0.000267	0.000338
$P_{\rm rot}$	244	−3.432		
No $P_{\rm rot}$	458	−3.632	0.000620	6.28×10^{-6}

To estimate $L_{\rm bol}$, we interpolate on the PMS evolutionary tracks of Siess et al. (2000) to obtain the predicted $L_{\rm bol}$ for each star, given the mass and age estimates from Prisinzano et al. (2005) using these same evolutionary tracks.

Figure 14 shows the resulting $L_X/L_{\rm bol}$ of the NGC 6530 rotators as a function of rotation period. As a whole the sample shows a roughly constant $L_X/L_{\rm bol}$ at approximately the "saturation" value of $\log L_X/L_{\rm bol} \approx -3.3$ (e.g., Pizzolato et al. 2003). However, the most rapidly rotating stars appear to exhibit a systematically reduced $L_X/L_{\rm bol}$. To quantify this, we perform both a K-S test and a Student's t-test comparing the $L_X/L_{\rm bol}$ for rapid rotators with $P < 2.5$ days versus more slowly rotating stars with $P > 2.5$ days (see Table 7). We find a statistically significant difference from both tests, with the mean $\log L_X/L_{\rm bol}$ for the rapid rotators (−3.56) being lower than that for the slower rotators (−3.37) with a statistical significance of 99.97%.

In addition, we have checked whether our sample of rotators is representative of the underlying population of NGC 6530 members in $L_X/L_{\rm bol}$. Figure 15 compares the distribution of $L_X/L_{\rm bol}$ for stars with and without a measured rotation period. We again find a very statistically significant difference in the two distributions from both a K-S test and a t-test. The mean

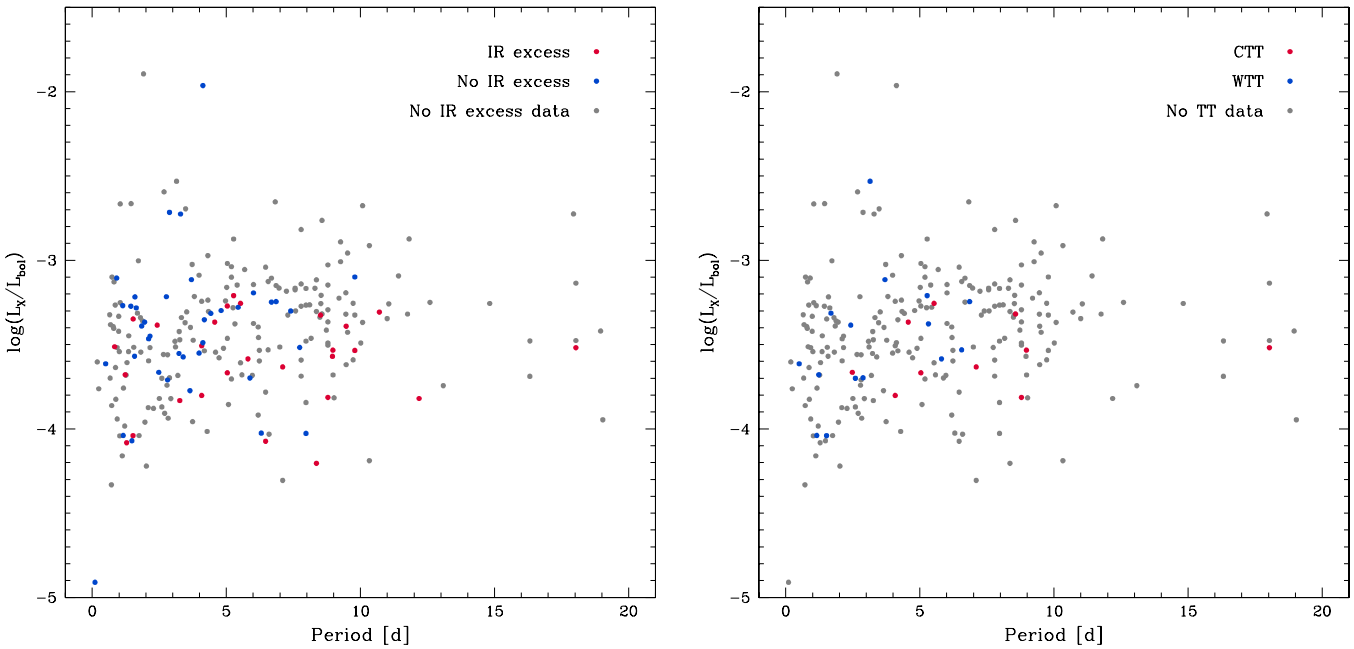

Figure 14. $L_X/L_{\rm bol}$ vs. rotation period for our sample of rotators in NGC 6530. Left: red points are those stars identified as having NIR excess in the Q_{VIJK} index (Damiani et al. 2006), blue points are those with no NIR excess, and gray points are those with no NIR classification. Right: red points are those stars identified as CTTSs, blue points are WTTSs (Prisinzano et al. 2007; Arias et al. 2007), and gray points are those with no Hα spectrum. A K-S test and a Student's t-test both show a statistically significant tendency for the most rapidly rotating stars to have lower $L_X/L_{\rm bol}$ (see Table 7), suggestive of the so-called super-saturation (e.g., James et al. 2000).

(A color version of this figure is available in the online journal.)

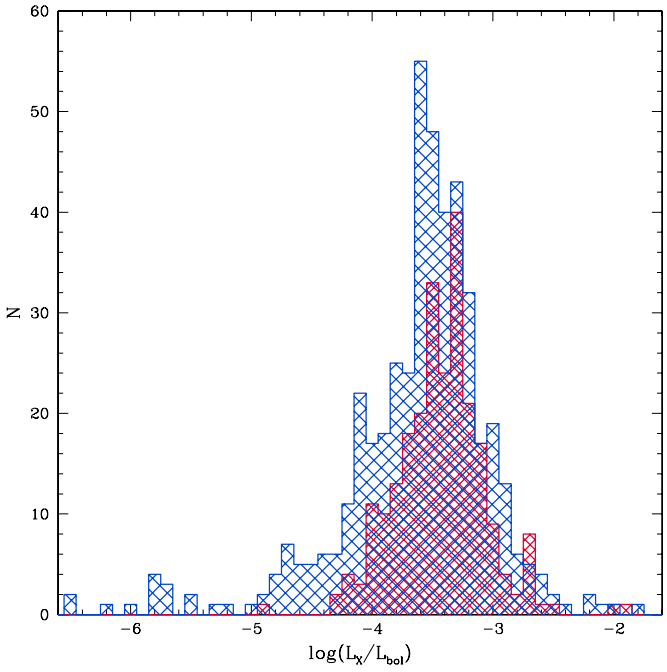

Figure 15. Red shaded histogram represents $L_X/L_{\rm bol}$ for NGC 6530 stars with rotation periods and the blue hatched histogram represents $L_X/L_{\rm bol}$ for those without rotation periods. Stars with rotation periods have significantly higher $L_X/L_{\rm bol}$ on average than those without detected periods (see Table 7).

(A color version of this figure is available in the online journal.)

log $L_X/L_{\rm bol}$ for the sample of rotators (−3.43) is significantly higher than that for the sample without detected rotation periods (−3.63). The probability that there is no difference in the mean log $L_X/L_{\rm bol}$ of the two samples is 6×10^{-6} (see Table 7).

5. DISCUSSION

Ever since the pioneering efforts of Bouvier and collaborators to measure rotation periods of Tau–Aur stars (e.g., Bouvier et al. 1986, 1993, 1997), and of Herbst and collaborators to measure rotation periods of ONC stars (e.g., Attridge & Herbst 1992; Herbst et al. 1994; Choi & Herbst 1996), a fundamental goal has been to characterize the morphology of the rotation period distribution for young low-mass stars. Early works on the ONC emphasized the apparent bimodality of the period distribution, with peaks around ∼2 days and ∼8 days and a deep gap in the distribution around ∼4–5 days (e.g., Attridge & Herbst 1992). In contrast, Stassun et al. (1999) found a unimodal distribution in the ONC. These differing results were subsequently argued to be a manifestation of the mass dependence of the period distribution (e.g., Herbst et al. 2001): a bimodal period distribution for solar-mass stars, a unimodal distribution for lower mass stars, and with the lower mass stars rotating faster than the higher mass stars. Several studies have confirmed these trends in the ONC and in other, slightly older clusters, including NGC 2264, NGC 2362, and IC 348 (e.g., Kearns et al. 1997; Kearns & Herbst 1998; Herbst et al. 2000; Lamm et al. 2005; Cieza & Baliber 2006; Irwin et al. 2008a). Thus, a picture has emerged in which young stars at $\gtrsim$1 Myr exhibit a mass-dependent period distribution that is bimodal at higher masses, in which lower mass stars rotate faster on average, and in which older stars tend to spin faster, presumably due to spin-up as the stars contract toward the main sequence.

The distribution of rotation periods we have measured for NGC 6530 is consistent with a uniform distribution for 0.5 days $< P <$ 10 days; we do not observe obvious bimodality in the period distribution. When we subdivide the sample stars into groups by mass, we do not observe bimodality among the higher mass stars (nor for the lower mass stars), and moreover

the lower mass stars rotate more slowly on average. These features of the NGC 6530 period distribution and its dependence on stellar mass differ strongly from the trends discussed above for numerous other clusters with ages $\gtrsim$1 Myr.

We find that NGC 6530 stars with older isochrone ages rotate more slowly on average than their younger counterparts. The statistical significance of this trend is not strong, but as with the other rotational properties of NGC 6530 noted above, such a trend is in contrast with that expected from the longer-term evolution observed between other extensively studied young clusters, which show a tendency for stars to spin up modestly between the age of the ONC and that of the Pleiades.

These differences in rotational characteristics between NGC 6530 and the other young clusters might be understood if NGC 6530 represents a population of PMS stars that is significantly younger than the other clusters, such that in particular the higher mass stars in the cluster are having their period distribution shaped from a unimodal one into a bimodal one, and the lowest mass stars in the cluster are actively spinning up so that they will end up spinning faster than their higher mass counterparts. That is, the NGC 6530 stars are perhaps currently evolving toward an evolutionary state when their rotational properties would presumably resemble those of the ONC. Indeed, the age of NGC 6530 has been estimated by Mayne et al. (2007) to be similar to, and possibly slightly younger than, the ONC.

In an attempt to more firmly place NGC 6530 in an evolutionary context relative to other well-studied young clusters, and motivated by the findings of Irwin et al. (2008a) who suggested patterns with age in the mass–period relationship of young clusters, we show in Figure 16 the rotation periods as a function of stellar mass for NGC 6530 and five other young clusters with extant rotation period measurements. NGC 6530 is shown first, and the other clusters ordered chronologically with ages from Mayne et al. (2007) and Mayne & Naylor (2008). Finally, we also include the zero-age main-sequence cluster NGC 2516. The six clusters from ONC to NGC 2516 thus span a range of ages from ∼2 Myr to ∼150 Myr. The period–mass relationship for NGC 6530 as expected appears most similar to that seen in the ONC. Broadly speaking, whereas the older clusters exhibit an increasing tendency for the upper envelope of rotation periods to slope downward at low stellar masses, the upper envelope of rotation periods in NGC 6530 is, like the ONC's, roughly flat with stellar mass. However, whereas the ONC does exhibit a modest downward slope toward decreasing stellar masses (i.e., the lowest mass stars in the ONC rotate on average faster than the higher mass stars), in NGC 6530 the trend is in the opposite sense (i.e., the lowest mass stars rotate on average more slowly; see Section 4.3), and this appears in Figure 16 as a slightly upward slope in the upper envelope of NGC 6530 rotation periods.

To better quantify these trends of rotation period with mass, we fit a linear trend line to the upper envelopes of the rotation periods versus mass for each of the clusters in Figure 16 (shown as red lines) as follows. For stars with masses in the range $0.5 < M/M_{\odot} < 0.1$, we grouped the stars into mass bins 0.1 $M_{\odot}$ wide, and within each of these mass bins we calculated the rotation period corresponding to the 75th percentile of the rotation periods in that bin. (We chose the 75th percentile because it is a more robust measure of the upper envelope of the distribution than, e.g., taking the uppermost data point in the bin.) We calculated the uncertainty on the 75th percentile periods as the difference between the 75th percentile and the 50th percentile (the median) divided by the square root of the number of data points in the bin. Finally, we fit a linear least-squares relationship to the binned points of the form $\log P = a \times M + b$, where a and b are free parameters of the fit. The resulting slopes a and their formal uncertainties are plotted versus the age of each cluster in Figure 17, in which we see a clear relationship of increasing slope with increasing age for the younger clusters with ages $\lesssim$10 Myr and a flattening of the relationship for the two oldest clusters at $\gtrsim$40 Myr. For specificity, the ages we assigned to each cluster are from Mayne & Naylor (2008, cf. their Table 9), except that for NGC 2362 we adopted an age of 3.5 Myr because its age was estimated as 3 Myr (Mayne & Naylor 2008) and 4 Myr (Mayne et al. 2007), and for IC348 we adopted 4.5 Myr as its age was estimated by Mayne & Naylor (2008) as 4–5 Myr. These cluster ages are summarized in Table 8.

For our linear fit in Figure 17 (solid line) we did not include NGC 6530; rather, we placed the point corresponding to NGC 6530 at the age at which the 1σ upper limit for its rotation period versus mass slope exactly lies on the linear trend fitted to the other clusters. The maximum age inferred for NGC 6530 by this procedure is 1.65 Myr, as compared to the 2 Myr age assigned to the ONC. In addition, the fit to the younger clusters was extended to only 6 Myr, as the measurements for the two

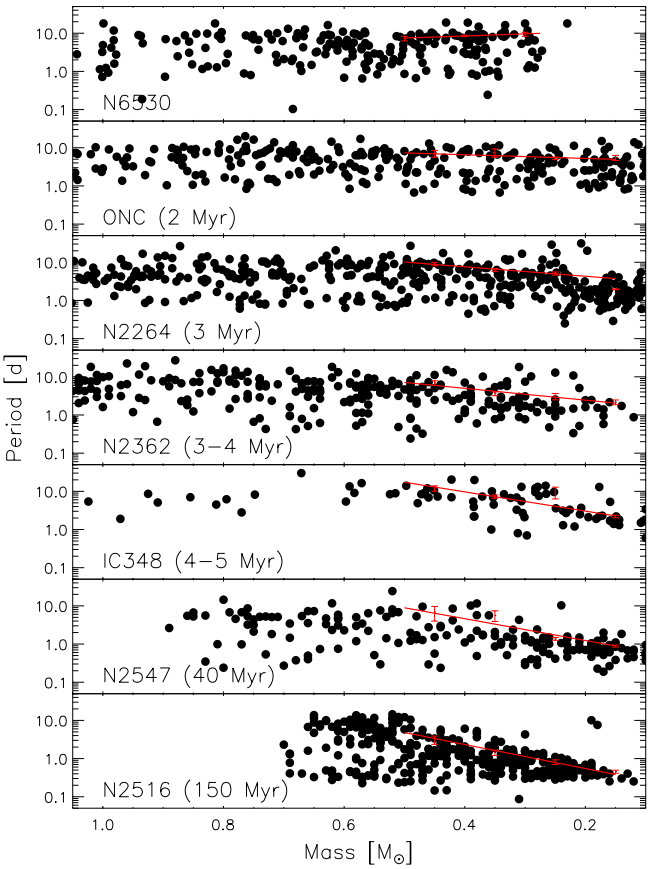

Figure 16. Rotation period as a function of mass for (top to bottom): NGC 6530, the ONC, NGC 2264, NGC 2362, IC 348, NGC 2547, and NGC 2516. Periods and masses for all clusters except NGC 6530 and IC 348 are from the compilation of Irwin et al. (2008a), with masses determined via interpolation on the PMS evolutionary tracks of Siess et al. (2000). Periods for IC 348 are from Cieza & Baliber (2006) and we derived masses using data from that paper by interpolating on the Siess et al. (2000) tracks. Periods and masses for NGC 6530 are from the present study. Solid lines in each panel represent a least-squares fit to the 75th percentile upper envelope of periods in each 0.1 $M_{\odot}$ mass bin for masses in the range 0.1–0.5 $M_{\odot}$, except for NGC 6530 which is limited to the range 0.2–0.5 $M_{\odot}$ (see Section 5 for discussion of this figure).

(A color version of this figure is available in the online journal.)

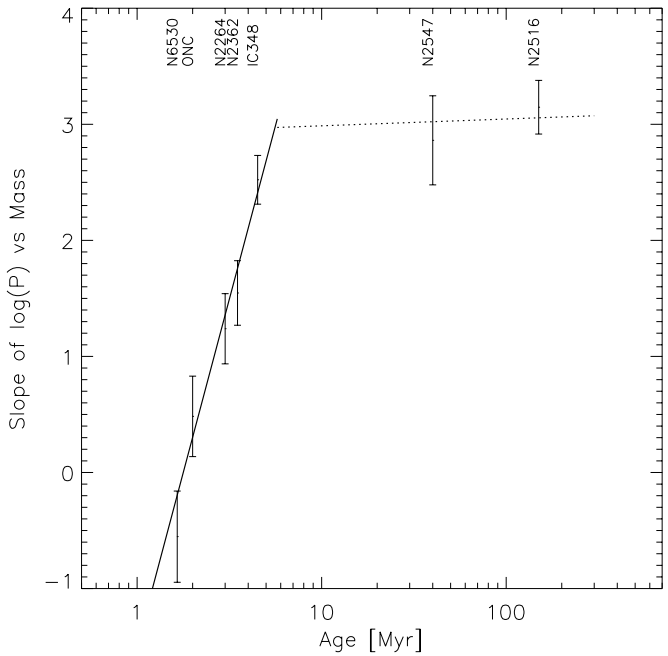

Figure 17. Slopes of the mass–period relationships from Figure 16 vs. cluster age. Cluster ages are from Mayne et al. (2007) and Mayne & Naylor (2008), except for NGC 6530 whose age was adjusted here to be consistent with the linear relationship (solid line) fitted to the ONC, NGC 2264, NGC 2362, and IC 348. The maximum age inferred for NGC 6530 is 1.65 Myr, on an age scale where the ONC is 2 Myr. See Section 5 for discussion of this figure.

oldest clusters (NGC 2547 and NGC 2516) clearly indicate that the trend of increasing slope in the period–mass plane with age must flatten at approximately this age (represented by the dotted line in Figure 17). The linear relationship fitted to the younger clusters (solid line in Figure 17) has the form

$$a = 5.98(\pm 1.11) \times \tau - 1.50(\pm 0.61), \quad (1)$$

where a is the slope of the linear relationship between log P (in days) and M (in $M_{\odot}$) for the upper 75th percentile of rotation periods in each cluster over the mass range 0.1–0.5 $M_{\odot}$, and τ is the cluster age (in Myr). This relationship may be useful for assigning relative ages to PMS stars on the basis of the observed slope in the period–mass relationship.

If NGC 6530 is indeed younger than the ONC, then this implies that the distance to the cluster of 1.25 kpc determined by Prisinzano et al. (2005) must be slightly underestimated. The median age of the stars in our sample inferred from the PMS isochrones of Siess et al. (2000) is ∼2 Myr (see Figures 3 and 8(b)), the same as the ONC using these isochrones. However, if the distance to NGC 6530 is taken to be just 15% larger, the median age of the NGC 6530 sample comes in line with our estimate of ∼1.5 Myr above. Prisinzano et al. (2005) do not quote an uncertainty on their distance determination, but most other recent distance estimates for the cluster are ∼25% larger than 1.25 kpc (e.g., van den Ancker et al. 1997; Loktin et al. 1997; Sung et al. 2000), so a 15% revision would not appear to be unreasonable. Indeed, the original X-ray study of Damiani et al. (2004) adopted a distance of 1.8 kpc, and consequently, determined a median age for the cluster of just 0.8 Myr from the same PMS isochrones used here (Siess et al. 2000).

The NGC 6530 rotation period distribution shows a strong cutoff for fast rotation periods, $P < 0.5$ days, and we have found that this short-period cutoff corresponds to breakup speed for these stars. A similar short-period cutoff associated with rotation

Table 8
Slopes of the Period–mass Relationship for Young Clusters

Cluster	Age (Myr)	Slope
N6530	1.65	-0.55 ± 0.39
ONC	2	0.48 ± 0.35
N2264	3	1.24 ± 0.30
N2362	3.5	1.55 ± 0.28
IC348	4.5	2.52 ± 0.21
N2547	40	2.86 ± 0.38
N2516	150	3.15 ± 0.23

Notes. Slopes are from linear fits to the upper envelope of rotation periods vs. mass, of the form $\log P = a \times M + b$, where P is in days and M is in $M_{\odot}$. Ages are from Mayne et al. (2007) and Mayne & Naylor (2008), except for NGC 6530 whose age here is determined from the linear relationship fitted to the other clusters. See Section 5.

at breakup was observed in the ONC (Stassun et al. 1999). A few stars in our sample are found with $P < 0.5$ days. While rotation at breakup is a possibility for these stars, we note that their light curves are strikingly similar to those of contact binaries. Some of these stars do have prior spectroscopic data in the literature that did not clearly identify them as spectroscopic binaries (see Table 4). However, we note that the spectra of contact binaries can appear highly broadened, and the line splitting might not be readily recognized as such. The discovery of PMS contact binaries would be very significant in the context of binary formation and evolution, and we suggest that these stars be monitored further for indications of radial velocity variations. A few PMS contact binary candidates have also been identified in Orion (Stassun et al. 1999; Rebull 2001; van Eyken et al. 2011).

The X-ray luminosities of the NGC 6530 stars are flat with rotation period, at the saturation level ($\log L_X/L_{\rm bol} \approx -3.3$; Pizzolato et al. 2003); however, the most rapidly rotating stars show significantly lower $\log L_X/L_{\rm bol}$ suggestive of the so-called super-saturation (e.g., James et al. 2000). A similar result was found in the ONC by Stassun et al. (2004a). Recent studies of rotation and X-ray activity in low-mass stars at a variety of ages (e.g., Wright et al. 2011; Jeffries et al. 2011) have argued that super-saturation may be the result of the X-ray coronae in very rapidly rotating stars extending beyond the Keplerian corotation radius, causing the coronae to be centrifugally stripped. To examine this idea in the context of our NGC 6530 sample, in Figure 18 we plot $\log L_X/L_{\rm bol}$ versus the Keplerian corotation radius ($R_{\rm co}$) for our sample, where $R_{\rm co}$ is determined for each star from the measured rotation period and from the mass and radius inferred from the Siess et al. (2000) evolutionary tracks. We find strong evidence for a correlation between these quantities, (shown as the line in Figure 18), similar to that suggested by Wright et al. (2011). A non-parametric Kendall's τ rank correlation test yields a positive correlation coefficient of 0.21, and the probability that the two quantities are not correlated is $<10^{-6}$. The fastest rotators in our NGC 6530 sample—and those with the lowest $L_X/L_{\rm bol}$ on average—have $R_{\rm co}$ in the range of 1–3 $R_{\star}$, whereas the slower rotators in our sample have $R_{\rm co}$ up to ∼15 $R_{\star}$. The COUP survey (Getman et al. 2005b) found that the coronae of low-mass PMS stars in that study, as inferred from the lengths of the magnetic loops driving the observed powerful X-ray flares, can have extents of up to ∼10 $R_{\star}$ (Favata et al. 2005; Aarnio et al. 2010). Such coronal radii can be accomodated within $R_{\rm co}$ for the slower rotators in our NGC 6530

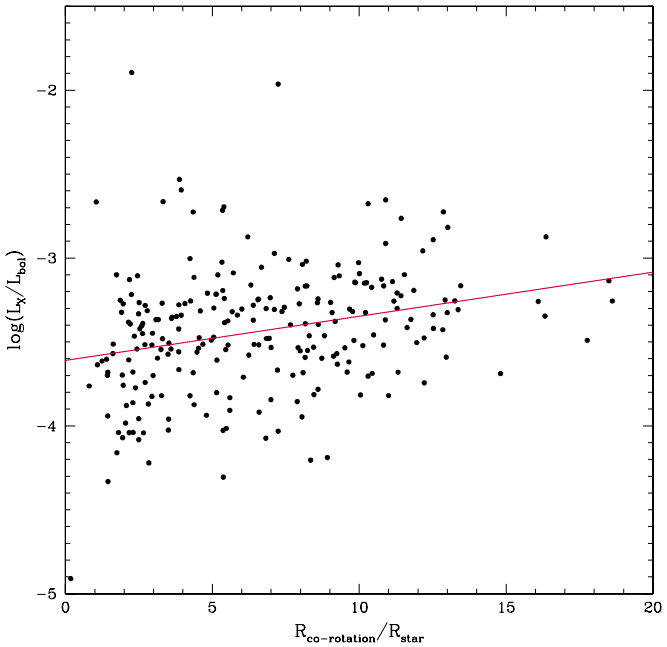

Figure 18. $\log(L_X/L_{\rm bol})$ vs. $R_{\rm co}/R_\star$ for NGC 6530 stars with rotation periods. The line represents a linear best fit of the form $\log(L_X/L_{\rm bol}) = 0.026(\pm0.006) \times R_{\rm co}/R_\star - 3.61(\pm0.05)$. A Kendall's τ test shows the trend to be highly statistically significant. This suggests that centrifugal stripping of the stellar coronae may be responsible for the super-saturation effect observed in Figure 14 (see also Wright et al. 2011).

(A color version of this figure is available in the online journal.)

sample, but for the faster rotators would extend beyond $R_{\rm co}$ and would thus be unlikely to remain stable against centrifugal forces. Thus, it appears plausible that the correlation we observe between $L_X/L_{\rm bol}$ and $R_{\rm co}$ is the result of the outer coronae of the rapidly rotating stars being increasingly centrifugally stripped, as suggested by Wright et al. (2011) and Jeffries et al. (2011).

Stassun et al. (2004a) also found in the ONC that stars with measured rotation periods exhibit significantly higher $L_X/L_{\rm bol}$ on average than ONC stars without rotation periods, and suggested that this might indicate a population of stars rotating more slowly than the observed long-period cutoff in the ONC ($P \gtrsim 10$ days). Our NGC 6530 sample exhibits very similar properties. In particular, we observe a long-period cutoff for $P \gtrsim 10$ days, and moreover we find that NGC 6530 stars that do not exhibit a rotation period signal in our data are less X-ray luminous on average. Perhaps there is a population of more slowly rotating stars in NGC 6530 than our rotation period measurements can reveal. These low L_X stars could still have periodic signals below 0.02 mag amplitudes that we would not detect given the precision of our data (see Section 3.1). Sensitive $v \sin i$ measurements in NGC 6530 and the ONC are needed to explore this possibility further.

We find evidence that stars in our NGC 6530 sample with NIR excess emission and/or strong Hα emission rotate more slowly on average. In other young clusters, an association between NIR excess and slow rotation has been taken as evidence of the braking of stellar rotation through a magnetic star–disk interaction (so-called disk-locking). However, it is not clear that disk-locking models actually predict such a correlation of increased NIR excess for slow rotators. A central prediction of most disk-locking models is that the location of the inner truncation radius of the circumstellar disk relative to the corotation radius determines the magnitude and sign of the torque experienced by the star. Thus for slow rotators, whose corotation radii are large and for which a braking torque would therefore require an even larger inner truncation radius, one might predict less NIR emission for the slow rotators due to the large inner hole in the disk (e.g., Stassun et al. 2001).

Le Blanc et al. (2011) performed detailed modeling of the spectral energy distributions of stars in IC 348 with measured rotation periods in order to assess in detail for each star the location of the inner disk edge relative to corotation. Those authors found that the slow rotators in IC 348 tended to possess disks with inner truncation radii at or beyond corotation, whereas the rapidly rotating stars tended to posses disks with inner truncation radii within corotation, implying that if star–disk interaction is important for the stars then it must be operating with a tendency to torque down the slow rotators and torque up the rapid rotators. In other words, if disks are important for angular momentum evolution in that cluster, then they must be important for stars at all rotation periods, spinning down some stars while spinning up others. Thus, inferring the nature of any star–disk interaction among our sample of rotators in NGC 6530 awaits detailed modeling of the spectral energy distributions of the stars in order to establish whether and how disks may be sculpting the NGC 6530 rotation period distribution.

6. SUMMARY AND CONCLUSIONS

We have photometrically monitored ∼50,000 stars in a $40' \times 40'$ field centered on NGC 6530, the young massive star-forming cluster illuminating the Lagoon Nebula, over 35 nights in the I_C band with a cadence of 1 hr^{-1}. These observations are intended to complement recent optical, X-ray, and NIR surveys of the region (Damiani et al. 2004; Prisinzano et al. 2005; Damiani et al. 2006; Prisinzano et al. 2007), permitting a comprehensive characterization of the young stellar population in NGC 6530.

From an analysis of periodic variations in our light curves, we measured rotation periods for 290 X-ray-selected cluster members of NGC 6530, with masses in the range $0.2 < M/M_\odot < 2.0$. From the findings of Damiani et al. (2004), we expect ∼5% of our catalog to be contaminated by non-members, or only ∼15 stars in our full photometric catalog. We investigated correlations between rotation period and other stellar properties, including mass, age, spatial distribution within the cluster, the presence of circumstellar disks, and X-ray activity. The major findings of this work are as follows.

1. The distribution of rotation periods in NGC 6530 is approximately uniform over the range 0.5 days $< P <$ 10 days; we do not observe obvious bimodality in the period distribution, regardless of whether the distribution is considered in its entirety or limited to narrower ranges of stellar mass. The sharp cutoff in the period distribution at $P \approx 0.5$ days likely results from the breakup limit for the stars in our sample. A small number of stars with $P < 0.5$ days are present, which should be investigated further as possible PMS contact binary systems.
2. The X-ray luminosities of the stars are roughly flat with rotation period, at approximately the saturation level ($\log L_X/L_{\rm bol} \approx -3.3$). However, the fastest rotators show lower average X-ray luminosities, at a highly statistically significant level, suggestive of the so-called super-saturation. At the same time, X-ray luminosity correlates most strongly with the stars' corotation radii, suggesting

that centrifugal stripping of the coronae may be the fundamental driver of the super-saturation phenomenon.

3. Stars with NIR excesses and Hα emission indicative of warm circumstellar material rotate more slowly on average than stars lacking disk signatures. Disked stars might be presumed to be younger on average, and indeed we find evidence that stars with younger ages as inferred from spatial location within the cluster rotate more slowly on average. However, the statistical significance is low, and indeed we find the opposite association between rotation and age when the ages are inferred from PMS isochrones.
4. The rotation periods are a function of stellar mass: the lower mass stars rotate more slowly on average than the higher mass stars. This is in the opposite sense of the period–mass relationship observed in the ONC and in all other slightly older clusters.
5. We show that the slope of the mass–period relationship among slow rotators (defined as the 75th percentile rotation periods) in the mass range $0.1 < M/M_{\odot} < 0.5$ is a good proxy for the age of a young cluster. Calibrating this empirical-mass–period–age relation to the ONC, NGC 2264, NGC 2362, IC348, NGC 2547, and NGC 2516, we find that NGC 6530 is the youngest of all, with a maximum age of 1.65 Myr on an age scale where the ONC is 2 Myr.

The evidence points strongly to NGC 6530 being in a very early stage of rotational evolution in which the stars are currently evolving toward a state that will presumably resemble the ONC within the next $\lesssim$1 Myr. Thus, NGC 6530 becomes an important new touchstone for theoretical models of angular momentum evolution in young, low-mass stars.

An important question that remains to be resolved is the role of circumstellar disks in the rotational evolution of these stars. The observed correlation between NIR excess and slow rotation has been taken in previous studies as evidence for rotational braking via star–disk interaction. However, it is not clear that theories of star–disk interaction in fact predict this correlation. Additionally, recent detailed modeling of the full spectral energy distributions of young stars with rotation periods in IC348 indicate that, if disks do affect the spin rates of the stars, they must act both to spin down some stars and to spin up others (Le Blanc et al. 2011). A similarly detailed assessment of the disk torques likely being experienced by the stars in NGC 6530 will be important to determine whether and how disks may yet be acting to shape the mass–period relationship in this very young cluster.

Finally, it remains an important challenge to empirically connect the rotational properties of PMS stars to those of main-sequence stars, and to theoretically connect the dominant mechanisms thought to govern the evolution of angular momentum in the PMS to those on the main sequence. Main-sequence angular momentum evolution is principally understood through intrinsic structural changes in the stars that, through stellar winds, lead to distinct period–mass relationships that evolve predictably with time and thus permit reliable age-dating of stars (gyrochronology). In contrast, in the PMS phase the dominant angular momentum evolution mechanisms have generally been thought to be extrinsic to the stars (e.g., disk-locking). Yet it is now clear that low-mass stars already evince clear period–mass relationships in the PMS stage. Evidently, as early as the very young age of NGC 6530, a period–mass relationship that can be projected forward to the main sequence is already taking form, and this relationship already encodes stellar age.

We thank Robert Siverd for technical assistance and Soeren Meibom for enlightening discussions. C.B.H. acknowledges the support of the NSF Graduate Research Fellowship 2011082275 and also the NSF-funded Research Experiences for Undergraduates program in Physics and Astronomy at Vanderbilt University. K.G.S. acknowledges support through NSF Grant AST-0808072, as well as the generous support and hospitality of a Martin Luther King Visiting Professorship at the Massachusetts Institute of Technology.

REFERENCES

Aarnio, A. N., Stassun, K. G., Hughes, W. J., & McGregor, S. L. 2011, Sol. Phys., 268, 195
Aarnio, A. N., Stassun, K. G., & Matt, S. P. 2009, in AIP Conf. Ser. 1094, Cool Stars, Stellar Systems and the Sun, ed. E. Stempels (Melville, NY: AIP), 337
Aarnio, A. N., Stassun, K. G., & Matt, S. P. 2010, ApJ, 717, 93
Allain, S., Bouvier, J., Prosser, C., Marschall, L. A., & Laaksonen, B. D. 1996, A&A, 305, 498
Arias, J. I., Barbá, R. H., & Morrell, N. I. 2007, MNRAS, 374, 1253
Aspin, C. 2011, AJ, 142, 135
Aspin, C., Barbieri, C., Boschi, F., et al. 2006, AJ, 132, 1298
Attridge, J. M., & Herbst, W. 1992, ApJ, 398, L61
Barnes, S. A. 2003, ApJ, 586, 464
Barnes, S. A. 2007, ApJ, 669, 1167
Barnes, S. A. 2010, ApJ, 722, 222
Barnes, S. A., & Kim, Y.-C. 2010, ApJ, 721, 675
Barnes, S. A., Sofia, S., Prosser, C. F., & Stauffer, J. R. 1999, ApJ, 516, 263
Basri, G., Johns-Krull, C. M., & Mathieu, R. D. 1997, AJ, 114, 781
Bastien, F. A., Stassun, K. G., & Weintraub, D. A. 2011, AJ, 142, 141
Bouvier, J., Alencar, S. H. P., Harries, T. J., Johns-Krull, C. M., & Romanova, M. M. 2007, in Protostars and Planets V, ed. B. Reipurth, D. Jewitt, & K. Keil (Tucson, AZ: Univ. Arizona Press), 479
Bouvier, J., Bertout, C., Benz, W., & Mayor, M. 1986, A&A, 165, 110
Bouvier, J., Cabrit, S., Fernandez, M., Martin, E. L., & Matthews, J. M. 1993, A&A, 272, 176
Bouvier, J., Chelli, A., Allain, S., et al. 1999, A&A, 349, 619
Bouvier, J., Dougados, C., & Alencar, S. H. P. 2004, Ap&SS, 292, 659
Bouvier, J., Grankin, K. N., Alencar, S. H. P., et al. 2003, A&A, 409, 169
Bouvier, J., Wichmann, R., Grankin, K., et al. 1997, A&A, 318, 495
Briceño, C., Vivas, A. K., Hernández, J., et al. 2004, ApJ, 606, L123
Casey, B. W., Mathieu, R. D., Vaz, L. P. R., Andersen, J., & Suntzeff, N. B. 1998, AJ, 115, 1617
Choi, P. I., & Herbst, W. 1996, AJ, 111, 283
Cieza, L., & Baliber, N. 2006, ApJ, 649, 862
Covey, K. R., Hillenbrand, L. A., Miller, A. A., et al. 2011, AJ, 141, 40
Covino, E., Catalano, S., Frasca, A., et al. 2000, A&A, 361, L49
Damiani, F., Flaccomio, E., Micela, G., et al. 2004, ApJ, 608, 781
Damiani, F., Prisinzano, L., Micela, G., & Sciortino, S. 2006, A&A, 459, 477
Da Rio, N., Robberto, M., Soderblom, D. R., et al. 2010, ApJ, 722, 1092
Favata, F., Flaccomio, E., Reale, F., et al. 2005, ApJS, 160, 469
Feigelson, E., Townsley, L., Güdel, M., & Stassun, K. 2007, in Protostars and Planets V, ed. B. Reipurth, D. Jewitt, & K. Keil (Tucson, AZ: Univ. Arizona Press), 313
Feigelson, E. D., Garmire, G. P., & Pravdo, S. H. 2002, ApJ, 572, 335
Feigelson, E. D., Getman, K., Townsley, L., et al. 2005, ApJS, 160, 379
Feigelson, E. D., Getman, K. V., Townsley, L. K., et al. 2011, ApJS, 194, 9
Getman, K. V., Feigelson, E. D., Grosso, N., et al. 2005a, ApJS, 160, 353
Getman, K. V., Flaccomio, E., Broos, P. S., et al. 2005b, ApJS, 160, 319
Gómez Maqueo Chew, Y., Stassun, K. G., Prša, A., & Mathieu, R. D. 2009, ApJ, 699, 1196
Grosso, N., Feigelson, E. D., Getman, K. V., et al. 2005, ApJS, 160, 530
Güdel, M., Briggs, K. R., Arzner, K., et al. 2007, A&A, 468, 353
Guenther, D. B., Kallinger, T., Zwintz, K., Weiss, W. W., & Tanner, J. 2007, ApJ, 671, 581
Gullbring, E., & Gahm, G. F. 1996, A&A, 308, 821
Güver, T., & Özel, F. 2009, MNRAS, 400, 2050
Hartman, J. D., Gaudi, B. S., Holman, M. J., et al. 2008, ApJ, 675, 1254
Hartmann, L., Hewett, R., Stahler, S., & Mathieu, R. D. 1986, ApJ, 309, 275
Hebb, L., Stempels, H. C., Aigrain, S., et al. 2010, A&A, 522, A37
Herbst, W., Bailer-Jones, C. A. L., & Mundt, R. 2001, ApJ, 554, L197
Herbst, W., Bailer-Jones, C. A. L., Mundt, R., Meisenheimer, K., & Wackermann, R. 2002, A&A, 396, 513

Herbst, W., Eislöffel, J., Mundt, R., & Scholz, A. 2007, in Protostars and Planets V, ed. B. Reipurth, D. Jewitt, & K. Keil (Tucson, AZ: Univ. Arizona Press), 297
Herbst, W., Hamilton, C. M., Leduc, K., et al. 2008, Nature, 452, 194
Herbst, W., Herbst, D. K., Grossman, E. J., & Weinstein, D. 1994, AJ, 108, 1906
Herbst, W., LeDuc, K., Hamilton, C. M., et al. 2010, AJ, 140, 2025
Herbst, W., Maley, J. A., & Williams, E. C. 2000, AJ, 120, 349
Hillenbrand, L. A. 1997, AJ, 113, 1733
Honeycutt, R. K. 1992, PASP, 104, 435
Irwin, J., Aigrain, S., Hodgkin, S., et al. 2007, MNRAS, 380, 541
Irwin, J., Hodgkin, S., Aigrain, S., et al. 2008a, MNRAS, 384, 675
Irwin, J., Hodgkin, S., Aigrain, S., et al. 2008b, MNRAS, 383, 1588
James, D. J., Jardine, M. M., Jeffries, R. D., et al. 2000, MNRAS, 318, 1217
Jeffries, R. D., Jackson, R. J., Briggs, K. R., Evans, P. A., & Pye, J. P. 2011, MNRAS, 411, 2099
Jensen, E. L. N., Dhital, S., Stassun, K. G., et al. 2007, AJ, 134, 241
Kastner, J. H., Richmond, M., Grosso, N., et al. 2004, Nature, 430, 429
Kearns, K. E., Eaton, N. L., Herbst, W., & Mazzurco, C. J. 1997, AJ, 114, 1098
Kearns, K. E., & Herbst, W. 1998, AJ, 116, 261
Kenyon, S. J., & Hartmann, L. 1995, ApJS, 101, 117
Koenigl, A. 1991, ApJ, 370, L39
Krishnamurthi, A., Terndrup, D. M., Pinsonneault, M. H., et al. 1998, ApJ, 493, 914
Lada, C. J., Gottlieb, C. A., Gottlieb, E. W., & Gull, T. R. 1976, ApJ, 203, 159
Lamm, M. H., Mundt, R., Bailer-Jones, C. A. L., & Herbst, W. 2005, A&A, 430, 1005
Lang, D., Hogg, D. W., Mierle, K., Blanton, M., & Roweis, S. 2010, AJ, 139, 1782
Le Blanc, T. S., Covey, K. R., & Stassun, K. G. 2011, AJ, 142, 55
Loktin, A., Zakharova, P., Gerasimenko, T., & Malisheva, L. 1997, Balt. Astron., 6, 316
Lomb, N. R. 1976, Ap&SS, 39, 447
Makidon, R. B., Rebull, L. M., Strom, S. E., Adams, M. T., & Patten, B. M. 2004, AJ, 127, 2228
Mathieu, R. D., Stassun, K., Basri, G., et al. 1997, AJ, 113, 1841
Matt, S., & Pudritz, R. E. 2004, ApJ, 607, L43
Matt, S., & Pudritz, R. E. 2005a, ApJ, 632, L135
Matt, S., & Pudritz, R. E. 2005b, MNRAS, 356, 167
Matt, S., & Pudritz, R. E. 2008a, ApJ, 678, 1109
Matt, S., & Pudritz, R. E. 2008b, ApJ, 681, 391
Mayne, N. J., & Naylor, T. 2008, MNRAS, 386, 261
Mayne, N. J., Naylor, T., Littlefair, S. P., Saunders, E. S., & Jeffries, R. D. 2007, MNRAS, 375, 1220
Menten, K. M., Reid, M. J., Forbrich, J., & Brunthaler, A. 2007, A&A, 474, 515
Mohanty, S., Stassun, K. G., & Doppmann, G. W. 2010, ApJ, 722, 1138
Mohanty, S., Stassun, K. G., & Mathieu, R. D. 2009, ApJ, 697, 713
Najita, J. 1995, RevMexAA, 27, 293
Ostriker, E. C., & Shu, F. H. 1995, ApJ, 447, 813
Patten, B. M., & Simon, T. 1996, ApJS, 106, 489
Pizzolato, N., Maggio, A., Micela, G., Sciortino, S., & Ventura, P. 2003, A&A, 397, 147
Press, W. H., & Rybicki, G. B. 1989, ApJ, 338, 277
Press, W. H., Teukolsky, S. A., Vetterling, W. T., & Flannery, B. P. 1992, in Numerical Recipes in C. The Art of Scientific Computing, ed. W. H. Press, S. A. Teukolsky, W. T. Vetterling, & B. P. Flannery (2nd ed.; Cambridge: Cambridge Univ. Press)
Prisinzano, L., Damiani, F., Micela, G., & Pillitteri, I. 2007, A&A, 462, 123
Prisinzano, L., Damiani, F., Micela, G., & Sciortino, S. 2005, A&A, 430, 941
Radick, R. R., Skiff, B. A., & Lockwood, G. W. 1990, ApJ, 353, 524
Radick, R. R., Thompson, D. T., Lockwood, G. W., Duncan, D. K., & Baggett, W. E. 1987, ApJ, 321, 459
Rebull, L. M. 2001, AJ, 121, 1676
Scargle, J. D. 1982, ApJ, 263, 835
Shu, F., Najita, J., Ostriker, E., et al. 1994, ApJ, 429, 781
Siess, L., Dufour, E., & Forestini, M. 2000, A&A, 358, 593
Stassun, K., & Wood, K. 1999, ApJ, 510, 892
Stassun, K. G., Ardila, D. R., Barsony, M., Basri, G., & Mathieu, R. D. 2004a, AJ, 127, 3537
Stassun, K. G., Hebb, L., López-Morales, M., & Prša, A. 2009, in IAU Symp. 258, The Ages of Stars, ed. E. E. Mamajek, D. R. Soderblom, & R. F. G. Wyse (Cambridge: Cambridge Univ. Press), 161
Stassun, K. G., Mathieu, R. D., Cargile, P. A., et al. 2008, Nature, 453, 1079
Stassun, K. G., Mathieu, R. D., Mazeh, T., & Vrba, F. J. 1999, AJ, 117, 2941
Stassun, K. G., Mathieu, R. D., & Valenti, J. A. 2006a, Nature, 440, 311
Stassun, K. G., Mathieu, R. D., & Valenti, J. A. 2007a, ApJ, 664, 1154
Stassun, K. G., Mathieu, R. D., Vaz, L. P. R., Stroud, N., & Vrba, F. J. 2004b, ApJS, 151, 357
Stassun, K. G., Mathieu, R. D., Vrba, F. J., Mazeh, T., & Henden, A. 2001, AJ, 121, 1003
Stassun, K. G., & Terndrup, D. 2003, PASP, 115, 505
Stassun, K. G., van den Berg, M., & Feigelson, E. 2007b, ApJ, 660, 704
Stassun, K. G., van den Berg, M., Feigelson, E., & Flaccomio, E. 2006b, ApJ, 649, 914
Stassun, K. G., van den Berg, M., Mathieu, R. D., & Verbunt, F. 2002, A&A, 382, 899
Stauffer, J. R., & Hartmann, L. W. 1987, ApJ, 318, 337
Stempels, H. C., Hebb, L., Stassun, K. G., et al. 2008, A&A, 481, 747
Sung, H., Chun, M.-Y., & Bessell, M. S. 2000, AJ, 120, 333
van den Ancker, M. E., The, P. S., Feinstein, A., et al. 1997, A&AS, 123, 63
van Eyken, J. C., Ciardi, D. R., Rebull, L. M., et al. 2011, AJ, 142, 60
Vogel, S. N., & Kuhi, L. V. 1981, ApJ, 245, 960
Walter, F. M., Neff, J. E., Gibson, D. M., et al. 1987, A&A, 186, 241
Walter, F. M., Stringfellow, G. S., Sherry, W. H., & Field-Pollatou, A. 2004, AJ, 128, 1872
Winn, J. N., Hamilton, C. M., Herbst, W. J., et al. 2006, ApJ, 644, 510
Wright, N. J., Drake, J. J., Mamajek, E. E., & Henry, G. W. 2011, ApJ, 743, 48
Zwintz, K., & Weiss, W. W. 2006, A&A, 457, 237